30 nM using Lipofectamine RNAiMAX (Invitrogen) in accordance with the manufacturer's instructions. Target sequences of the siRNAs were: occludin (5′-GCAAGAUCACUAUGAGACA-3′), SR-BI (5′-GAGCUUUGGCCUUGGUCUA-3′), CD81 (5′-CUGUGAUCAUGAUCUUCGA-3′), CHC (5′-CUAGCUUUGCACAGUUUAA-3′), Dyn2 (5′-CCCUCAAGGAGGCGCUCAA-3′), Cav1 (5′-CCCUAAACACCUCAACGAU-3′), flotillin-1 (5′-CCUAUGACAUCGAGGUCAA-3′), Arf6 (5′-CAGUUCUUGGUAAAGUCCU-3′), CtBP1 (5′-GACUCGACGCUGUGCCACA-3′) and PAK1 (5′-GCAUCAAUUCCUGAAGAUU-3′). Target sequences of the siRNAs for claudin-1, PI4K and scrambled negative control were as described previously (Suzuki *et al.*, 2013).

Immunoblotting. Cells were washed with PBS and incubated with passive lysis buffer (Promega). Lysates were sonicated for 10 min and added to the same volume of 2 × SDS-PAGE sample buffer. Protein samples were boiled for 10 min, separated by SDS-PAGE and then transferred to PVDF membranes (Merck Millipore). After blocking, membranes were probed with primary antibodies, followed by incubation with peroxidase-conjugated secondary antibody. Antigen–antibody complexes were visualized using an enhanced chemiluminescence detection system (SuperSignal West Pico Chemiluminescent Substrate; Thermo Scientific) in accordance with the manufacturer's protocols.

Flow cytometry. Cultured cells detached by treatment with trypsin were incubated with anti-CD81 antibody or anti-mouse IgG antibody for 1 h at 4 °C. After being washed with PBS containing 0.1 % BSA, cells were incubated with an Alexa Fluor 488-conjugated anti-mouse secondary antibody (Invitrogen) for 1 h at 4 °C, washed repeatedly and resuspended in PBS. Analyses were performed using a FACSCalibur system (Becton Dickinson).

Reagents and antibodies. Bafilomycin A1 was obtained from Wako Pure Chemical Industries. Alexa Fluor 488-conjugated transferrin was obtained from Invitrogen. For immunoblotting, anti-SR-BI (NB400-104; Novus Biologicals), anti-occludin (71-1500; Invitrogen), anti-claudin-1 (51-9000; Invitrogen), anti-Dyn2 (ab3457; Abcam), anti-Cav1 (N-20; Santa Cruz Biotechnology), anti-flotillin (H-104; Santa Cruz Biotechnology), anti-Arf6 (ab77581; Abcam) and anti-PAK1 (2602; Cell Signaling Technology) rabbit polyclonal antibodies; anti-CD81 (JS-81; BD Biosciences), anti-β-actin (AC-15; Sigma-Aldrich), anti-CHC (23; BD Biosciences), anti-GRAF1 (SAB1400439; Sigma-Aldrich) and anti-glyceraldehyde 3-phosphate dehydrogenase (6C5; Merck Millipore) mouse mAb; and anti-CtBP1 goat polyclonal antibody (C-17; Santa Cruz Biotechnology) were used. For immunofluorescence staining, anti-CHC mAb (X22) and anti-HA rat polyclonal antibody (3F10) were obtained from Thermo Scientific and Roche Applied Science, respectively. Anti-NS5A antibody was a rabbit polyclonal antibody against synthetic peptides. Alexa Fluor 488- or 555-labelled secondary antibodies were obtained from Invitrogen.

DNA transfection. Cell monolayers were transfected with plasmid DNA using TransIT-LT1 transfection reagent (Mirus) in accordance with the manufacturer's instructions.

Treatment of cells with bafilomycin A1 and cell viability. Cells were preincubated with various concentrations of bafilomycin A1 for 60 min at 37 °C. Preincubated cells were then infected with HCVtcp. Cells treated with 0.1 % DMSO were used as controls. Cell viability was analysed by the Cell Titre-Glo Luminescent Cell Viability Assay (Promega).

Uptake of transferrin. Cells were grown on glass coverslips. After cells were transfected with HA-tagged Dyn2 expression plasmids, Alexa Fluor 488-conjugated transferrin at 20 $\mu g\ ml^{-1}$ was added and incubated for 30 min. Cells were washed with PBS and fixed in 4 % paraformaldehyde.

Immunofluorescence analysis. Huh7.5.1 and Huh-7 cells were fixed with 4 % paraformaldehyde in PBS for 30 min, and were then blocked and permeabilized with 0.3 % Triton X-100 in a non-fat milk solution (Block Ace; Snow Brand Milk Products) for 60 min at room temperature. Samples were then incubated with anti-CHC, anti-Dyn2, anti-Cav1, anti-NS5A or anti-HA for 60 min at room temperature, washed three times with PBS, and then incubated with secondary antibodies for 60 min at room temperature. Finally, samples were washed three times with PBS, rinsed briefly in double-distilled H_2O and mounted with DAPI mounting medium. The signal was analysed using a Leica TCS SPE confocal microscope.

Luciferase assay. For quantification of FLuc activity in HCVtcp-infected cells, cells were lysed with passive lysis buffer (Promega) at 72 h post-infection. FLuc activity of the cells was determined using a luciferase assay system (Promega). For quantification of GLuc activity in supernatants of HCVtcp-infected cells, the *Renilla* Luciferase Assay System (Promega) was used. All luciferase assays were performed at least in triplicate.

Quantification of HCV core protein. HCV core protein was quantified using a highly sensitive enzyme immunoassay (Lumipulse G1200; Fujirebio) in accordance with the manufacturer's instructions.

ACKNOWLEDGEMENTS

We are grateful to Francis V. Chisari (Scripps Research Institute) for providing Huh-7 and Huh7.5.1 cells. We would also like to thank M. Sasaki for technical assistance, and T. Kato, A. Murayama and K. Mori for helpful discussion.

REFERENCES

Acosta, E. G., Castilla, V. & Damonte, E. B. (2008). Functional entry of dengue virus into *Aedes albopictus* mosquito cells is dependent on clathrin-mediated endocytosis. *J Gen Virol* **89**, 474–484.

Acosta, E. G., Castilla, V. & Damonte, E. B. (2009). Alternative infectious entry pathways for dengue virus serotypes into mammalian cells. *Cell Microbiol* **11**, 1533–1549.

Akazawa, D., Date, T., Morikawa, K., Murayama, A., Omi, N., Takahashi, H., Nakamura, N., Ishii, K., Suzuki, T. & other authors (2008). Characterization of infectious hepatitis C virus from liver-derived cell lines. *Biochem Biophys Res Commun* **377**, 747–751.

Bartosch, B., Vitelli, A., Granier, C., Goujon, C., Dubuisson, J., Pascale, S., Scarselli, E., Cortese, R., Nicosia, A. & Cosset, F. L. (2003). Cell entry of hepatitis C virus requires a set of co-receptors that include the CD81 tetraspanin and the SR-B1 scavenger receptor. *J Bio Chem* **278**, 41624–41630.

Benedicto, I., Molina-Jimenez, F., Bartosch, B., Cosset, F. L., Lavillette, D., Prieto, J., Moreno-Otero, R., Valenzuela-Fernandez, A., Aldabe, R., Lopez-Cabrera, M. & Majano, P. L. (2009). The tight junction-associated protein occludin is required for a postbinding step in hepatitis C virus entry and infection. *J Virol* **83**, 8012–8020.

Blanchard, E., Belouzard, S., Goueslain, L., Wakita, T., Dubuisson, J., Wychowski, C. & Rouillé, Y. (2006). Hepatitis C virus entry depends on clathrin-mediated endocytosis. *J Virol* **80**, 6964–6972.

Blight, K. J., McKeating, J. A. & Rice, C. M. (2002). Highly permissive cell lines for subgenomic and genomic hepatitis C virus RNA replication. *J Virol* **76**, 13001–13014.

Codran, A., Royer, C., Jaeck, D., Bastien-Valle, M., Baumert, T. F., Kieny, M. P., Pereira, C. A. & Martin, J. P. (2006). Entry of hepatitis C

virus pseudotypes into primary human hepatocytes by clathrin-dependent endocytosis. *J Gen Virol* **87**, 2583–2593.

Coller, K. E., Berger, K. L., Heaton, N. S., Cooper, J. D., Yoon, R. & Randall, G. (2009). RNA interference and single particle tracking analysis of hepatitis C virus endocytosis. *PLoS Pathog* **5**, e1000702.

Damke, H., Baba, T., van der Bliek, A. M. & Schmid, S. L. (1995). Clathrin-independent pinocytosis is induced in cells overexpressing a temperature-sensitive mutant of dynamin. *J Cell Biol* **131**, 69–80.

Damm, E. M., Pelkmans, L., Kartenbeck, J., Mezzacasa, A., Kurzchalia, T. & Helenius, A. (2005). Clathrin- and caveolin-1-independent endocytosis: entry of simian virus 40 into cells devoid of caveolae. *J Cell Biol* **168**, 477–488.

Evans, M. J., von Hahn, T., Tscherne, D. M., Syder, A. J., Panis, M., Wolk, B., Hatziioannou, T., McKeating, J. A., Bieniasz, P. D. & Rice, C. M. (2007). Claudin-1 is a hepatitis C virus co-receptor required for a late step in entry. *Nature* **446**, 801–805.

Grove, J. & Marsh, M. (2011). The cell biology of receptor-mediated virus entry. *J Cell Biol* **195**, 1071–1082.

Grove, J., Nielsen, S., Zhong, J., Bassendine, M. F., Drummer, H. E., Balfe, P. & McKeating, J. A. (2008). Identification of a residue in hepatitis C virus E2 glycoprotein that determines scavenger receptor BI and CD81 receptor dependency and sensitivity to neutralizing antibodies. *J Virol* **82**, 12020–12029.

Helle, F., Vieyres, G., Elkrief, L., Popescu, C.-I., Wychowski, C., Descamps, V., Castelain, S., Roingeard, P., Duverlie, G. & Dubuisson, J. (2010). Role of N-linked glycans in the functions of hepatitis C virus envelope proteins incorporated into infectious virions. *J Virol* **84**, 11905–11915.

Hoofnagle, J. H. (2002). Course and outcome of hepatitis C. *Hepatology* **36** (Suppl 1), S21–S29.

Kambara, H., Fukuhara, T., Shiokawa, M., Ono, C., Ohara, Y., Kamitani, W. & Matsuura, Y. (2012). Establishment of a novel permissive cell line for the propagation of hepatitis C virus by expression of microRNA miR122. *J Virol* **86**, 1382–1393.

Kataoka, C., Kaname, Y., Taguwa, S., Abe, T., Fukuhara, T., Tani, H., Moriishi, K. & Matsuura, Y. (2012). Baculovirus GP64-mediated entry into mammalian cells. *J Virol* **86**, 2610–2620.

Kato, N., Mori, K., Abe, K., Dansako, H., Kuroki, M., Ariumi, Y., Wakita, T. & Ikeda, M. (2009). Efficient replication systems for hepatitis C virus using a new human hepatoma cell line. *Virus Res* **146**, 41–50.

Liu, S., Yang, W., Shen, L., Turner, J. R., Coyne, C. B. & Wang, T. (2009). Tight junction proteins claudin-1 and occludin control hepatitis C virus entry and are downregulated during infection to prevent superinfection. *J Virol* **83**, 2011–2014.

Lupberger, J., Zeisel, M. B., Xiao, F., Thumann, C., Fofana, I., Zona, L., Davis, C., Mee, C. J., Turek, M. & other authors (2011). EGFR and EphA2 are host factors for hepatitis C virus entry and possible targets for antiviral therapy. *Nat Med* **17**, 589–595.

Marsh, M. & Helenius, A. (2006). Virus entry: open sesame. *Cell* **124**, 729–740.

Matlin, K. S., Reggio, H., Helenius, A. & Simons, K. (1981). Infectious entry pathway of influenza virus in a canine kidney cell line. *J Cell Biol* **91**, 601–613.

McKeating, J. A., Zhang, L. Q., Logvinoff, C., Flint, M., Zhang, J., Yu, J., Butera, D., Ho, D. D., Dustin, L. B., Rice, C. M. & Balfe, P. (2004). Diverse hepatitis C virus glycoproteins mediate viral infection in a CD81-dependent manner. *Journal of virology* **78**, 8496–8505.

Meertens, L., Bertaux, C. & Dragic, T. (2006). Hepatitis C virus entry requires a critical postinternalization step and delivery to early endosomes via clathrin-coated vesicles. *J Virol* **80**, 11571–11578.

Mercer, J., Schelhaas, M. & Helenius, A. (2010). Virus entry by endocytosis. *Annu Rev Biochem* **79**, 803–833.

Miaczynska, M. & Stenmark, H. (2008). Mechanisms and functions of endocytosis. *J Cell Biol* **180**, 7–11.

Mosso, C., Galván-Mendoza, I. J., Ludert, J. E. & del Angel, R. M. (2008). Endocytic pathway followed by dengue virus to infect the mosquito cell line C6/36 HT. *Virology* **378**, 193–199.

Norkin, L. C., Anderson, H. A., Wolfrom, S. A. & Oppenheim, A. (2002). Caveolar endocytosis of simian virus 40 is followed by brefeldin A-sensitive transport to the endoplasmic reticulum, where the virus disassembles. *J Virol* **76**, 5156–5166.

Pelkmans, L., Kartenbeck, J. & Helenius, A. (2001). Caveolar endocytosis of simian virus 40 reveals a new two-step vesicular-transport pathway to the ER. *Nat Cell Biol* **3**, 473–483.

Pileri, P., Uematsu, Y., Campagnoli, S., Galli, G., Falugi, F., Petracca, R., Weiner, A. J., Houghton, M., Rosa, D., Grandi, G. & Abrignani, S. (1998). Binding of hepatitis C virus to CD81. *Science* **282**, 938–941.

Ploss, A., Evans, M. J., Gaysinskaya, V. A., Panis, M., You, H., de Jong, Y. P. & Rice, C. M. (2009). Human occludin is a hepatitis C virus entry factor required for infection of mouse cells. *Nature* **457**, 882–886.

Sainz, B., Jr, Barretto, N., Martin, D. N., Hiraga, N., Imamura, M., Hussain, S., Marsh, K. A., Yu, X., Chayama, K. & other authors (2012). Identification of the Niemann–Pick C1-like 1 cholesterol absorption receptor as a new hepatitis C virus entry factor. *Nat Med* **18**, 281–285.

Scarselli, E., Ansuini, H., Cerino, R., Roccasecca, R. M., Acali, S., Filocamo, G., Traboni, C., Nicosia, A., Cortese, R. & Vitelli, A. (2002). The human scavenger receptor class B type I is a novel candidate receptor for the hepatitis C virus. *Embo J* **21**, 5017–5025.

Sieczkarski, S. B. & Whittaker, G. R. (2002a). Dissecting virus entry via endocytosis. *J Gen Virol* **83**, 1535–1545.

Sieczkarski, S. B. & Whittaker, G. R. (2002b). Influenza virus can enter and infect cells in the absence of clathrin-mediated endocytosis. *J Virol* **76**, 10455–10464.

Sumpter, R., Jr, Loo, Y.-M., Foy, E., Li, K., Yoneyama, M., Fujita, T., Lemon, S. M. & Gale, M., Jr (2005). Regulating intracellular antiviral defense and permissiveness to hepatitis C virus RNA replication through a cellular RNA helicase, RIG-I. *J Virol* **79**, 2689–2699.

Suzuki, T., Ishii, K., Aizaki, H. & Wakita, T. (2007). Hepatitis C viral life cycle. *Adv Drug Deliv Rev* **59**, 1200–1212.

Suzuki, R., Saito, K., Kato, T., Shirakura, M., Akazawa, D., Ishii, K., Aizaki, H., Kanegae, Y., Matsuura, Y. & other authors (2012). Trans-complemented hepatitis C virus particles as a versatile tool for study of virus assembly and infection. *Virology* **432**, 29–38.

Suzuki, R., Matsuda, M., Watashi, K., Aizaki, H., Matsuura, Y., Wakita, T. & Suzuki, T. (2013). Signal peptidase complex subunit 1 participates in the assembly of hepatitis C virus through an interaction with E2 and NS2. *PLoS Pathog* **9**, e1003589.

Trotard, M., Lepère-Douard, C., Régeard, M., Piquet-Pellorce, C., Lavillette, D., Cosset, F. L., Gripon, P. & Le Seyec, J. (2009). Kinases required in hepatitis C virus entry and replication highlighted by small interference RNA screening. *FASEB J* **23**, 3780–3789.

van der Schaar, H. M., Rust, M. J., Chen, C., van der Ende-Metselaar, H., Wilschut, J., Zhuang, X. & Smit, J. M. (2008). Dissecting the cell entry pathway of dengue virus by single-particle tracking in living cells. *PLoS Pathog* **4**, e1000244.

Vieyres, G., Thomas, X., Descamps, V., Duverlie, G., Patel, A. H. & Dubuisson, J. (2010). Characterization of the envelope glycoproteins associated with infectious hepatitis C virus. *J Virol* **84**, 10159–10168.

Zhong, J., Gastaminza, P., Cheng, G., Kapadia, S., Kato, T., Burton, D. R., Wieland, S. F., Uprichard, S. L., Wakita, T. & Chisari, F. V. (2005). Robust hepatitis C virus infection *in vitro*. *Proc Natl Acad Sci U S A* **102**, 9294–9299.

Biochemical and Biophysical Research Communications 452 (2014) 315–321

Contents lists available at ScienceDirect

Biochemical and Biophysical Research Communications

journal homepage: www.elsevier.com/locate/ybbrc

Formation of covalently closed circular DNA in Hep38.7-Tet cells, a tetracycline inducible hepatitis B virus expression cell line

Naoki Ogura [a], Koichi Watashi [b], Toru Noguchi [a], Takaji Wakita [b,*]

[a] Central Pharmaceutical Research Institute, Japan Tobacco Inc., Osaka, Japan
[b] Department of Virology II, National Institute of Infectious Diseases, Tokyo, Japan

ARTICLE INFO

Article history:
Received 17 July 2014
Available online 20 August 2014

Keywords:
HBV
cccDNA
Antiviral

ABSTRACT

Hepatitis B virus (HBV) covalently closed circular DNA (cccDNA) plays a central role in chronic HBV infection. However, analysis of the molecular mechanism of cccDNA formation is difficult because of the low efficiency in tissue cultured cells. In this study, we developed a more efficient cccDNA expression cell, Hep38.7-Tet, by subcloning from a tetracycline inducible HBV expression cell, HepAD38. Higher levels of cccDNA were produced in Hep38.7-Tet cells compared to HepAD38 cells. In Hep38.7-Tet cells, the cccDNA was detectable at six days after HBV induction. HBV e antigen (HBeAg) secretion was dependent upon cccDNA production. We screened chemical compounds using Hep38.7-Tet cells and HBeAg secretion as a marker. Most of the hit compounds have already been reported as anti-HBV compounds. These data suggested that Hep38.7-Tet cells will be powerful tools for analysis of the molecular mechanism of cccDNA formation/maintenance and development of novel therapeutic agents to control HBV infection.
© 2014 Elsevier Inc. All rights reserved.

1. Introduction

It is estimated that two billion people worldwide have been infected with hepatitis B virus (HBV) [1]. Chronic HBV infection is currently a major public health burden, affecting approximately 240 million individuals worldwide [2]. These patients have an elevated risk of chronic active hepatitis, cirrhosis or primary hepatocellular carcinoma [3–5].

Following HBV infection, the viral genomic relaxed circular DNA (rcDNA) is translocated into the cell nucleus and converted into episomal covalently closed circular DNA (cccDNA), which serves as a transcription template for viral mRNA. After transcription and nuclear export, cytoplasmic viral pregenomic RNA (pgRNA) is assembled by HBV polymerase and capsid proteins to form the nucleocapsid. Polymerase-catalyzed reverse transcription in the nucleocapsid yields minus-strand DNA, which is subsequently copied into plus-strand DNA to form the progeny rcDNA genome. Mature nucleocapsids are then either packaged with viral envelope proteins to egress as virion particles or shuttled back to the nucleus to amplify the cccDNA reservoir through the intracellular cccDNA amplification pathway [6–8].

Establishment of infection and viral persistence are both dependent on the formation of cccDNA during the HBV replication cycle [9–13]. The half-life of cccDNA is longer than other viral nucleic acids ranging from days to months in animal and tissue culture models [14–16]. Thus, there is an urgent need for the development of novel therapeutic agents that directly target cccDNA formation/maintenance. Formation of cccDNA in HepG2 cells transiently transfected with HBV genome is not efficient [17]. In HepAD38 cells, a tetracycline inducible HBV expression cell line, production of secreted HBV e antigen (HBeAg) is predominantly cccDNA dependent and thus might be useful as a surrogate marker of cccDNA formation [18–20]. To identify small molecules that inhibit cccDNA formation, we developed a more efficient cccDNA expression cell system. In the present study, we used Hep38.7-Tet cells subcloned from HepAD38 cells to investigate the levels of cccDNA formation, mRNA transcription, replication, viral particle secretion and HBeAg secretion.

2. Materials and methods

2.1. Cell culture

HepG2.2.15 [21] and HepG2.2.15.7 cells (unpublished data, M. Iwamoto and K. Watashi) were maintained in DMEM/F12 medium (Life Technologies, Carlsbad, CA) supplemented with 10% fetal bovine serum, 100 U/mL Penicillin, 100 μg/mL Streptomycin,

* Corresponding author. Address: Department of Virology II, National Institute of Infectious Diseases, 1-23-1 Toyama, Shinjuku-ku, Tokyo 162-8640, Japan. Fax: +81 3 5285 1161.
E-mail addresses: naoki.ogura@jt.com (N. Ogura), kwatashi@nih.go.jp (K. Watashi), toru.noguchi@jt.com (T. Noguchi), wakita@nih.go.jp (T. Wakita).

http://dx.doi.org/10.1016/j.bbrc.2014.08.029
0006-291X/© 2014 Elsevier Inc. All rights reserved.

400 μg/mL Geneticin and 5 μg/mL Insulin. HepAD38 (a gift from Dr. Christoph Seeger at Fox Chase Cancer Center) and Hep38.7-Tet cells were maintained in the same way as HepG2.2.15 cells but with the addition of 400 ng/mL tetracycline.

The cells were seeded onto 60 mm dishes at a density of 8.0×10^5 cells/well with tetracycline-containing medium. After 24 h incubation, tetracycline was removed from the medium to induce HBV replication. The plate was incubated for 6 days. The tetracycline was then added back to the medium to prevent HBV pgRNA transcription from integrated DNA [22]. HBV replication, cccDNA accumulation, pre-core mRNA transcription and HBeAg secretion were only induced from cccDNA formed in the 6 days without tetracycline. The plate was incubated for another 6 days. The cells and culture medium were harvested at indicated time points.

2.2. Compound sources

Entecavir was purchased from Wako Pure Chemical Industries, Ltd. CCC-0975 was synthesized at Japan Tobacco Inc. FDA approved drug screening library (Selleck Chemicals, Houston, TX) which consisted of 414 compounds in total. Compounds were dissolved in dimethyl sulfoxide (DMSO) to a concentration of 10 mM.

2.3. Compound screening

Hep38.7-Tet cells were seeded into 96-well plates at a density of 3.0×10^4 cells/well with tetracycline-containing medium. After 24 h incubation, tetracycline was removed from the medium and then compound-containing medium was added to screening plates at a final concentration of 10 μM in 0.1% DMSO. Screening plates were incubated for 6 days. Tetracycline was then added back to the medium and incubation continued for another 6 days. The activity of compounds was evaluated by measurement of secreted HBeAg in the medium. The cell viability was measured using the CellTiter 96 AQueous One Solution Cell Proliferation Assay (Promega, Japan).

2.4. Nucleic acid analysis

Intracellular core DNA was extracted as described previously [23,24]. Fifteen micrograms of extracted DNA was resolved by electrophoresis with a 1.2% agarose gel and transferred onto Hybond-XL membrane (GE Healthcare, Piscataway, NJ) in 20× SSC buffer. Total cellular RNA was extracted with TRIzol reagents (Life Technologies). Ten micrograms of total RNA were resolved in a 1.2% agarose gel containing 2.2 M formaldehyde and transferred onto Hybond-XL membrane. Extraction of cccDNA was carried out using a modified Hirt extraction procedure [25–28]. DNA (15 μg) was resolved and separated in a 1.2% agarose gel and transferred onto Hybond-XL membrane. For the detection of viral DNA and RNA, membranes were probed with full-length HBV DNA labeled with AlkPhos direct labeling reagents (GE Healthcare). After incubation with hybridization buffer for 6 h at 65 °C, the membrane was quantified by digital imaging with a LAS-4000 (GE Healthcare).

2.5. Viral particle assay

Viral particles (including virions, subviral particles and nucleocapsids) were extracted as described previously [29]. Viral particles in culture medium were precipitated by adding PEG8000 to a final concentration of 10% and incubated on ice for 1 h, followed by centrifugation at 8000 rpm at 4 °C for 10 min. Pellets were dissolved in TNE buffer.

2.6. Real-time PCR assay

Viral DNA was quantified using EXPRESS SYBR GreenER qPCR Supermix (Life Technologies). Core DNA and DNA containing particles selective primers were 5′-CTCGTGGTGGACTTCTCTC-3′ (Forward) and 5′-AAGATGAGGCATAGCAGCA-3′ (Reverse). Primers selective for cccDNA were 5′-CGTCTGTGCCTTCTCATCTGC-3′ (Forward) and 5′-GCACAGCTTGGAGGCTTGAA-3′ (Reverse). The cycling parameters were as follows: 50 °C for 2 min, 95 °C for 2 min, then 45 cycles of 95 °C for 15 s and 60 °C for 1 min with an Applied Biosystems 7500 sequence detection system (Life Technologies). The HBV plasmid was diluted over a range of 10^7–10^2 copies and used as a standard.

2.7. Real-time reverse transcription-PCR assay

Total RNA was extracted as described previously [20]. Five micrograms of total RNA extracted with TRIzol reagents were digested with 5 units RQ1 RNase-free DNase (Promega) and further purified with RNeasy mini kit (QIAGEN, Hilden, Germany). Synthesis of cDNA was from 1 μL purified total RNA using SuperScript III First-Strand Synthesis System (Life Technologies), based on the manufacturer's instruction. The selective primers used to transcribe cDNA from HBV RNA were 5′-GACCACCAAATGCCCCTATC-3′ (Forward) and 5′-GATTGAGATCTTCTGCGACGC-3′ (Reverse). The cycling parameters as described above.

2.8. Reverse transcription-PCR assay

The cDNA transcribed from pre-core RNA were quantified using PrimeSTAR Max DNA Polymerase (Takara, Japan). The primers were 5′-TAGGCATAAATTGGTCTG-3′ (Forward) and 5′-GATTGAGATCTTCTGCGACGC-3′ (Reverse). The cycling parameters were as follows: 94 °C for 1 min, then 45 cycles of 98 °C for 10 s, 55 °C for 5 s and 72 °C for 1 min. DNA was resolved and separated in a 1% agarose gel.

2.9. Indirect immunofluorescence analysis

Indirect immunofluorescence analysis was performed essentially as described previously [30,31]. Briefly, after fixation with 4% paraformaldehyde and permeabilization with 0.3% Triton-X-100, an anti-HBV core antibody (DAKO) was used as the primary antibody.

3. ELISA

The level of HBeAg in culture medium was measured using the HBe monoclonal ELISA kit (SIEMENS, Munich, Germany) according to the manufacturer's instructions.

4. Results

4.1. Intracellular cccDNA formation in HBV expression cell lines

We subcloned from HepAD38 cells and selected Hep38.7-Tet cells that showed the highest replication levels among the established subclones (unpublished data, M. Iwamoto and K. Watashi). We also subcloned HepG2.2.15.7 cells from HepG2.2.15 cells (unpublished data, M. Iwamoto and K. Watashi). To validate cccDNA levels in HBV expression cell lines, we compared cccDNA formation in tetracycline inducible Hep38.7-Tet, HepAD38 cells and non-inducible HepG2.2.15, HepG2.2.15.7 cells. As shown in Fig. 1, cccDNA could be detected after day 6 in all four cell lines. Hep38.7-Tet cells showed the highest levels of cccDNA

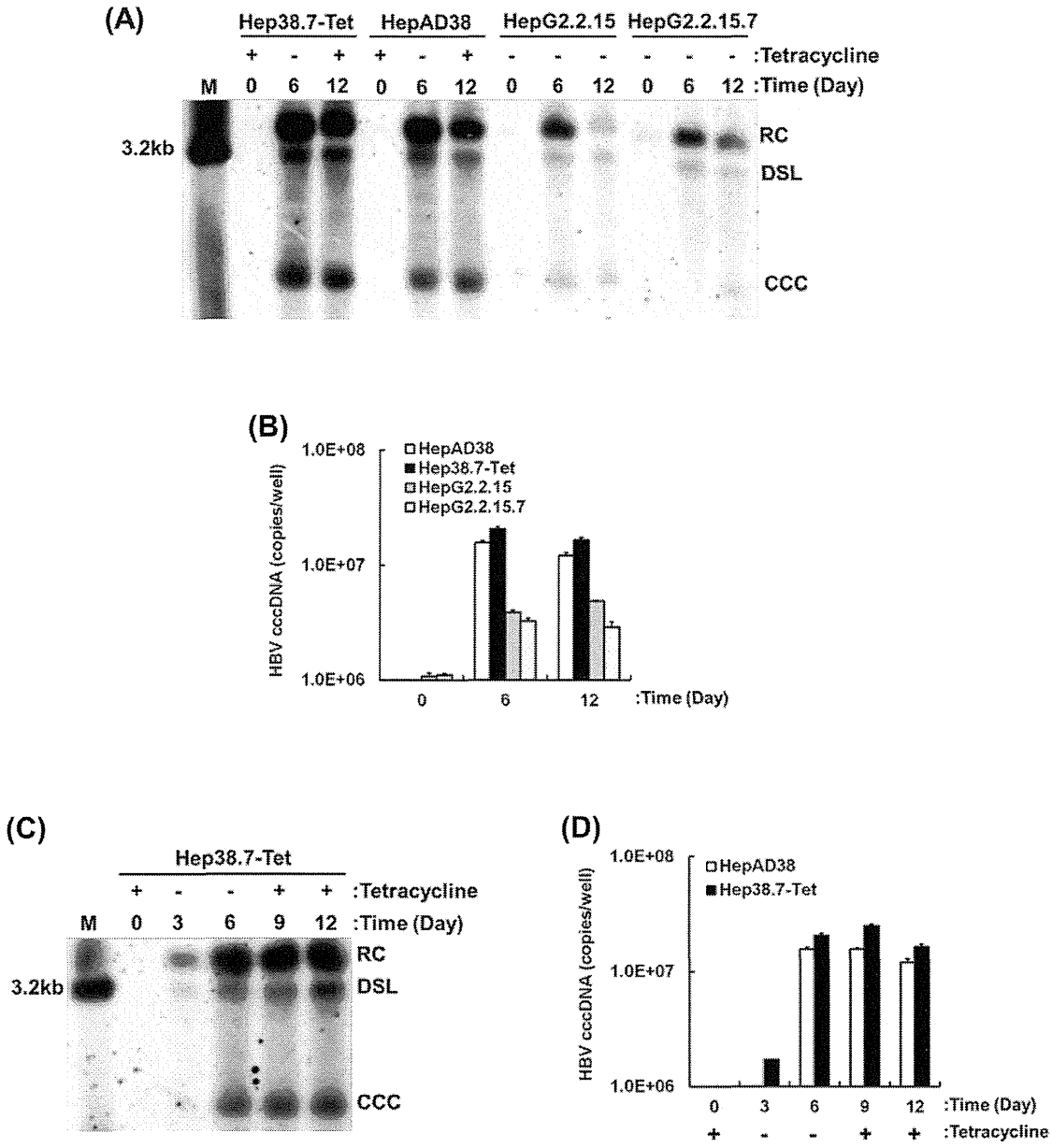

Fig. 1. Intracellular HBV cccDNA formation in Hep38.7-Tet cells. Hep38.7-Tet, HepAD38, HepG2.2.15 and HepG2.2.15.7 cells were harvested on days 0, 6 and 12. HBV cccDNA was extracted from the cells and analyzed by Southern blot (A) and Real-time PCR assay (B). Hep38.7-Tet and HepAD38 cells were harvested on days 0, 3, 6, 9 and 12. HBV cccDNA was extracted from the cells and analyzed by Southern blot (C) and Real-time PCR assay (D). Full length HBV DNA (3.2 kb) served as a control (lane M). The positions of relaxed circular DNA (RC), double stranded linear DNA (DSL) and covalently closed circular DNA (CCC) are indicated.

accumulation among the cell lines tested by Southern blot analysis and Real-time PCR assay (Fig. 1A and B). Higher levels of cccDNA were formed in tetracycline inducible cell lines compared to non-inducible cell lines.

4.2. Kinetics of intracellular cccDNA formation

We further investigated the kinetics of cccDNA levels after HBV induction in Hep38.7-Tet cells. The cells were seeded into 60 mm dishes with tetracycline-containing medium. After 24 h incubation, tetracycline was removed from the medium and the cells were cultured for 6 days. The tetracycline was then added back to the medium and incubation was continued for another 6 days. Southern blotting indicated that HBV cccDNA could be detected at day 6 and slowly increased from day 6 to day 12 (Fig. 1C). The accumulation of cccDNA in Hep38.7-Tet cells was higher than in HepAD38 cells at all timepoints examined (Fig. 1D). We calculated the copy number of cccDNA in Hep38.7-Tet cells from the results of the Real-time PCR assay. At day 3 cccDNA was present at 2 copies per cell and increased to 16 copies per cell at day 12. Liver biopsies have been shown to contain 1–50 copies of cccDNA per cell by Real-time PCR assay [32–35]. The copy number of cccDNA in Hep38.7-Tet cells was similar to that observed in HBV infected human hepatocytes.

4.3. Kinetics of intracellular HBV DNA synthesis

To determine HBV DNA replication in Hep38.7-Tet cells, we analyzed intracellular core DNA synthesis. As shown in Fig. 2, HBV core DNA could be detected by Southern blot analysis at day 3 and increased until day 12 (Fig. 2A). Using a Real-time PCR assay, core DNA synthesis in Hep38.7-Tet cells was found to be 2–4 times higher than in HepAD38 cells under similar conditions (Fig. 2B).

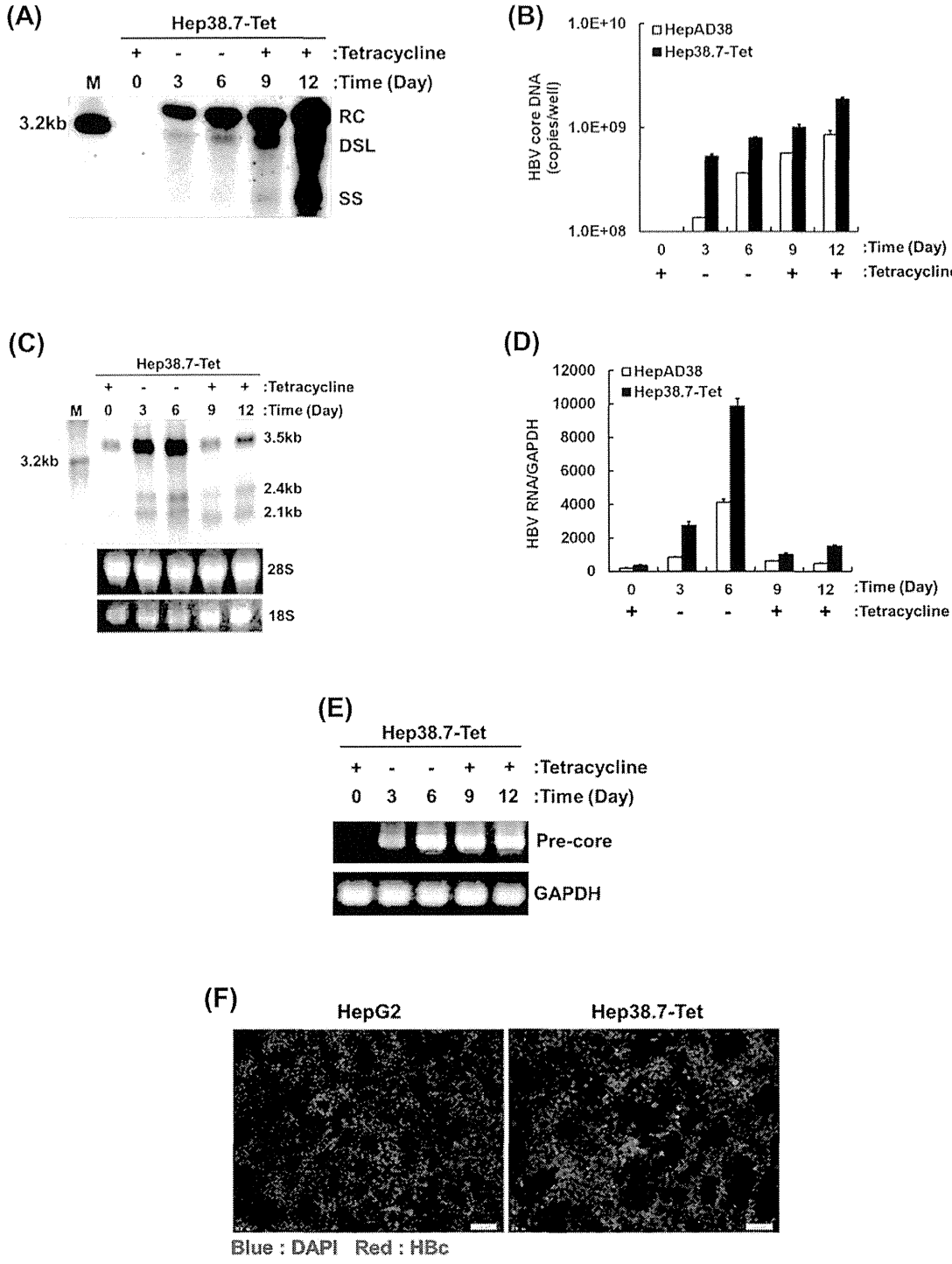

Fig. 2. Intracellular HBV core DNA synthesis, HBV mRNA transcription and HBc protein expression in Hep38.7-Tet cells. Hep38.7-Tet and HepAD38 cells were harvested on days 0, 3, 6, 9 and 12. HBV core DNA was extracted from the cells and analyzed by Southern blot (A) and Real-time PCR assay (B). Full length HBV DNA (3.2 kb) served as a control (lane M). The positions of relaxed circular DNA (RC), double stranded linear DNA (DSL) and single stranded DNA (SS) are indicated. Total cellular RNA was extracted and HBV RNA was detected by Northern blot (C) and Real-time reverse transcription-PCR assay (D). rRNA (28S and 18S) served as a loading control. The positions of HBV pgRNA (3.5 kb) and surface mRNAs (2.4 kb and 2.1 kb) are indicated. Pre-core mRNA was detected by Reverse transcription-PCR assay (E). GAPDH served as a loading control. By indirect immunofluorescence analysis, Hep38.7-Tet and HepG2 cells were stained for HBcAg on day 12 (F).

4.4. Pre-core mRNA transcription is cccDNA dependent

We next evaluated the synthesis of HBV RNA in Hep38.7-Tet cells. Northern blotting analysis showed that 3.5 kb HBV mRNA transcription increased until day 6 and then decreased following the addition of tetracycline (Fig. 2C). Using a Real-time reverse transcription-PCR assay, the transcription of HBV mRNA in Hep38.7-Tet cells was 2–3 times higher than in HepAD38 cells (Fig. 2D). These results implied that mRNA transcription, core DNA synthesis and cccDNA formation sequentially occurred during the HBV replication cycle in Hep38.7-Tet cells.

Because pre-core mRNA is only 35 nt longer than pgRNA, it is difficult to analyze by Northern blot and we therefore designed a pre-core mRNA specific reverse transcription-PCR assay. Using the same RNA samples shown in Fig. 2C, we found that the predicted reverse transcription-PCR product from pre-core mRNA

could be detected at day 3 and increased in parallel with cccDNA in the following 6 days (Fig. 2E). After the addition of tetracycline back into the medium, viral pgRNA and envelope mRNA, but not pre-core mRNA transcription declined from integrated viral DNA. This result suggested that pre-core mRNA was transcribed from cccDNA but not integrated viral DNA.

4.5. Intracellular HBc protein expression

To analyze the intracellular HBV protein expression, we evaluated HBc protein in the cell using a specific HBc antibody. The intracellular HBc protein was detected in Hep38.7-Tet cells but not HepG2 cells by indirect immunofluorescence analysis (Fig. 2F).

4.6. Kinetics of viral particle formation

To analyze viral particle formation, we evaluated the extracellular viral particles including virions and naked capsids. As shown in Fig. 3, extracellular HBV DNA in Hep38.7-Tet cells was higher than in HepAD38 cells indicating that virions and nucleocapsids were secreted into the medium (Fig. 3A).

4.7. Correlation of HBeAg secretion and cccDNA formation

To explore the possibility that HBeAg could serve as a reporter for formation of cccDNA, we measured the levels of its secretion in Hep38.7-Tet cells. ELISA results indicated that the levels of HBeAg increased until day 12. HBeAg secretion in Hep38.7-Tet cells was approximately twice that in HepAD38 cells (Fig. 3B). There was a good correlation between cccDNA formation and HBeAg secretion (Fig. 1C).

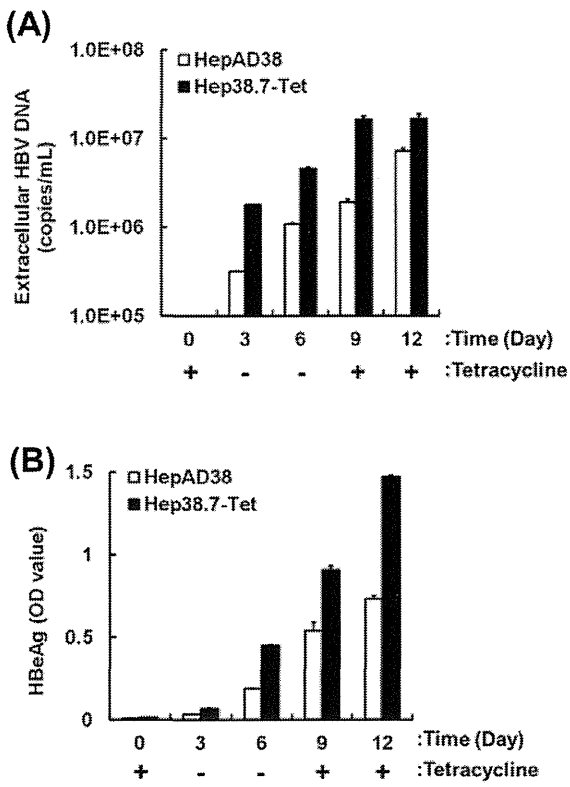

Fig. 3. Extracellular HBV DNA and HBeAg secretion in Hep38.7-Tet cells. Culture media of Hep38.7-Tet and HepAD38 cells were collected on days 0, 3, 6, 9 and 12. HBV particles (including virions and naked capsids) were precipitated by adding PEG8000 from the medium. HBV DNA was extracted from the HBV particles and analyzed by qPCR assay (A). HBeAg in culture medium was determined by ELISA (B).

4.8. Identification of anti-HBV compounds from Hep38.7-Tet cell-based assay

We evaluated the inhibitory activities of anti-HBV compounds, reverse transcriptase inhibitor (Entecavir) and cccDNA formation inhibitor (CCC-0975). Hep38.7-Tet cells were seeded into 96-well plates with tetracycline-containing medium. After 24 h incubation, tetracycline was removed from medium and then compound-containing medium was added to the screening plates. Screening plates were incubated for 6 days. Tetracycline was then added back to the medium and incubation continued for another 6 days. The activity of compounds was evaluated by measurement of secreted HBeAg in the medium at day 12. As shown in Fig. 4, these compounds had dose dependent inhibitions against cccDNA formation and showed similar inhibitory activities as previous reports [36,37]. The inhibition of cccDNA was proportional to the HBeAg reduction (Fig. 4A). Southern blot analysis showed that these compounds caused a dose dependent reduction of cccDNA (Fig. 4B). These results support the use of Hep38.7-Tet cells for screening to identify compounds that affect the HBV life cycle, including cccDNA formation.

Next, to identify compounds that affect cccDNA formation and maintenance, we screened chemical compound library at a final concentration of 10 μM. As shown in Table 1, CCC-0975 caused a 78% inhibition of HBeAg levels compared with control. Twelve compounds caused more than 50% inhibition of HBeAg levels without cytotoxicity for primary hits. These compounds included reverse transcriptase inhibitors, HMG-CoA reductase inhibitor, a steroid hormone, immunosuppressant agents and tetracycline.

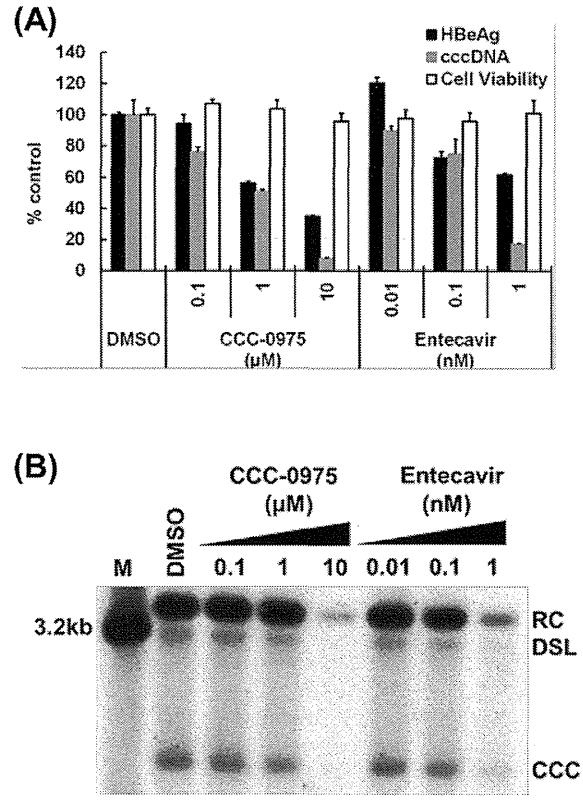

Fig. 4. Inhibitory activities of anti-HBV inhibitors in Hep38.7-Tet cells. Cells and culture medium were collected on day 12. HBV cccDNA was extracted from the cells and analyzed by Real-Time PCR assay. HBeAg in culture medium was determined by ELISA (A). HBV cccDNA was extracted from the cells and analyzed by Southern blotting (B). Full length HBV DNA (3.2 kb) served as a control (lane M). The positions of relaxed circular DNA (RC), double stranded linear DNA (DSL) and covalently closed circular DNA (CCC) are indicated.

Table 1
Antiviral activities of hit compounds.

Compound		HBeAg inhibition (% control)
Telbivudine	Reverse transcriptase inhibitor	24
Entecavir	Reverse transcriptase inhibitor	26
Tenofovir	Reverse transcriptase inhibitor	23
Emtricitabine	Reverse transcriptase inhibitor	29
Zalcitabine	Reverse transcriptase inhibitor	32
Nelarabine	Reverse transcriptase inhibitor	28
Pitavastatin	HMG-CoA reductase inhibitor	41
Progesterone	Steroid hormone	31
Mycophenolic	Immunosuppressant agent	32
Leflunomide	Immunosuppressant agent	24
Oxytetracycline	Tetracycline antibiotic	12
Methacycline	Tetracycline antibiotic	11
CCC-0975	cccDNA formation Inhibitor	22

Tenofovir and Entecavir are clinically used for HBV treatment [38]. Immunosuppressant agents have been reported to have anti-HBV activity [39]. Tetracycline antibiotics stopped HBV induction. These results indicate that Hep38.7-Tet cells are a suitable system to identify potential therapeutic agents.

5. Discussion

We subclones Hep38.7-Tet cells from HepAD38 cells which is a HepG2 derived cell line supporting tetracycline inducible HBV replication. Upon tetracycline withdrawal, the transcribed pgRNA will express viral core protein and polymerase and initiate reverse transcription to generate rcDNA. The start codon of the C-terminally truncated pre-core open reading frame (ORF) at the 3′ end of the pgRNA is copied into the viral DNA sequence and the pre-core ORF is restored during rcDNA conversion into cccDNA. Thus, the authentic pre-core mRNA will be transcribed only from cccDNA, with the translated pre-core protein being further processed into HBeAg, which is secreted into the culture medium and serves as a marker for cccDNA formation.

Hep38.7-Tet cells exhibited higher levels of HBV mRNA transcription, replication, cccDNA formation, virion secretion and HBeAg secretion than parental HepAD38 cells. These results may be due to the earlier transcription initiation of HBV pgRNA from integrated HBV after removal of tetracycline in Hep38.7-Tet cells than that in HepAD38 cells. We also confirmed that pre-core mRNA transcription was dependent on cccDNA formation and HBeAg secretion was quantitatively correlated with cccDNA formation. Moreover, the secreted HBeAg levels were sufficient to discover antiviral compounds in Hep38.7-Tet cells. In fact, we found some hits from the small-molecular compound library that significantly reduced the HBeAg levels. Many of these hit compounds had been identified as anti-HBV compounds previously. In this cell-based assay, any compounds that inhibit viral gene transcription, translation, HBeAg post-translational processing and secretion would be selected as positive hits. For example, CCC-0975 was discovered as an inhibitor of cccDNA production from a cccDNA-dependent HBeAg-producing cell line, HepDE19 [37]. This compound reduced the HBeAg levels in primary screening and reduced the levels of cccDNA and its putative precursor, deproteinized relaxed circular DNA (DP-rcDNA) in further mechanistic studies. Therefore, it is essential to evaluate the intracellular cccDNA levels in order to find a cccDNA inhibitor. Nevertheless, Hep38.7-Tet cells serve as a high throughput cell-based assay to identify cccDNA formation inhibitors. In conclusion, Hep38.7-Tet cells will be a powerful tool to analyze the molecular mechanism of HBV cccDNA formation and will facilitate the development of novel therapeutic agents for HBV infection.

Conflict of interest

No potential conflict of interest relevant to this article was reported.

Acknowledgments

This work was partially supported by Grants-in-Aid for Scientific Research from the Japan Society for the Promotion of Science, from the Ministry of Health, Labour and Welfare of Japan, from the Ministry of Education, Culture, Sports, Science and Technology of Japan. We thank Dr. Christoph Seeger (Fox Chase Cancer Center, Philadelphia, PA) for providing HepAD38 cell line. We gratefully acknowledge all members of the virus team at National Institute of Infectious Diseases (Tokyo, Japan) and Japan Tobacco Central Pharmaceutical Research Institute (Osaka, Japan).

References

[1] P. Ocama, C.K. Opio, W.M. Lee, Hepatitis B virus infection: current status, Am. J. Med. 118 (2005). 1413.e15–1413.e22.
[2] J.J. Ott, G.A. Stevens, J. Groeger, S.T. Wiersma, Global epidemiology of hepatitis B virus infection: new estimates of age-specific HBsAg seroprevalence and endemicity, Vaccine 30 (12) (2012) 2212–2219.
[3] T.M. Block, H. Guo, J.T. Guo, Molecular virology of hepatitis B virus for clinicians, Clin. Liver Dis. 11 (4) (2007) 685–706. vii.
[4] T.J. Liang, Hepatitis B: the virus and disease, Hepatology 49 (2009) S13–S21.
[5] B.J. McMahon, Epidemiology and natural history of hepatitis B, Semin. Liver Dis. 25 (Suppl. 1) (2005) 3–8.
[6] D. Ganem, H.E. Varmus, The molecular biology of the hepatitis B viruses, Annu. Rev. Biochem. 56 (1987) 651–693.
[7] M. Nassal, Hepatitis B viruses: reverse transcription a different way, Virus Res. 134 (1–2) (2008) 235–249.
[8] C. Seeger, W.S. Mason, Hepatitis B virus biology, Microbiol. Mol. Biol. Rev. 64 (1) (2000) 51–68.
[9] G. Moraleda, J. Saputelli, C.E. Aldrich, D. Averett, L. Condreay, W.S. Mason, Lack of effect of antiviral therapy in nondividing hepatocyte cultrures on the closed circular DNA of woodchuck hepatitis virus, J. Virol. 71 (12) (1997) 9392–9399.
[10] J. Summers, P.M. Smith, A.L. Horwich, Hepadnavirus envelope proteins regulate covalently closed circular DNA amplification, J. Virol. 64 (6) (1990) 2819–2824.
[11] J.S. Tuttleman, C. Pourcel, J. Summers, Formation of the pool of covalently closed circular viral DNA in hepadnavirus-infected cells, Cell 47 (3) (1986) 451–460.
[12] T.T. Wu, L. Coates, C.E. Aldrich, J. Summers, W.S. Mason, In hepatocytes infected with duck hepatitis B virus, the template for viral RNA synthesis is amplified by an intracellular pathway, Virology 175 (1) (1990) 255–261.
[13] Y.Y. Zhang, B.H. Zhang, D. Theele, S. Litwin, E. Toll, J. Summers, Single-cell analysis of covalently closed circular DNA copy numbers in a hepadnavirus-infected liver, Proc. Natl. Acad. Sci. U.S.A. 100 (21) (2003) 12372–12377.
[14] H. Guo, D. Jiang, T. Zhou, A. Cuconati, T.M. Block, J.T. Guo, Characterization of the intracellular deproteinized relaxed circular DNA of hepatitis B virus: an intermediate of covalently closed circular DNA formation, J. Virol. 81 (22) (2007) 12472–12484.
[15] Y. Zhu, T. Yamamoto, J. Cullen, J. Saputelli, C.E. Aldrich, D.S. Miller, S. Litwin, P.A. Furman, A.R. Jilbert, W.S. Mason, Kinetics of hepadnavirus loss from the liver during inhibition of viral DNA synthesis, J. Virol. 75 (1) (2001) 311–322.
[16] F. Zoulim, New insight on hepatitis B virus persistence from the study of intrahepatic viral cccDNA, J. Hepatol. 42 (3) (2005) 302–308.

[17] P.P. Scaglioni, M. Melegari, J.R. Wands, Posttranscriptional regulation of hepatitis B virus replication by the precore protein, J. Virol. 71 (1) (1997) 345–353.
[18] S.K. Ladner, M.J. Otto, C.S. Barker, K. Zaifert, G.H. Wang, J.T. Guo, C. Seeger, R.W. King, Inducible expression of human hepatitis B virus (HBV) in stably transfected hepatoblastoma cells: a novel system for screening potential inhibitors of HBV replication, Antimicrob. Agents Chemother. 41 (8) (1997) 1715–1720.
[19] J. Wang, A.S. Lee, J.H. Ou, Proteolytic conversion of hepatitis B virus e antigen precursor to end product occurs in a postendoplasmic reticulum compartment, J. Virol. 65 (9) (1991) 5080–5083.
[20] T. Zhou, H. Guo, J.T. Guo, A. Cuconati, A. Mehta, T.M. Block, Hepatitis B virus e antigen production is dependent upon covalently closed circular (ccc) DNA in HepAD38 cell cultures and may serve as a cccDNA surrogate in antiviral screening assays, Antiviral Res. 72 (2) (2006) 116–124.
[21] M.A. Sells, A.Z. Zelent, M. Shvartsman, G. Acs, Replicative intermediates of hepatitis B virus in HepG2 cells that produce infectious virions, J. Virol. 62 (8) (1988) 2836–2844.
[22] J.T. Guo, M. Pryce, X. Wang, M.I. Barrasa, J. Hu, C. Seeger, Conditional replication of duck hepatitis B virus in hepatoma cells, J. Virol. 77 (3) (2003) 1885–1893.
[23] H. Guo, W.S. Mason, C.E. Aldrich, J.R. Saputelli, D.S. Miller, A.R. Jilbert, J.E. Newbold, Identification and characterization of avihepadnaviruses isolated from exotic anseriformes maintained in captivity, J. Virol. 79 (5) (2005) 2729–2742.
[24] H. Guo, T. Zhou, D. Jiang, A. Cuconati, G.H. Xiao, T.M. Block, J.T. Guo, Regulation of hepatitis B virus replication by the phosphatidylinositol 3-kinase-akt signal transduction pathway, J. Virol. 81 (18) (2007) 10072–10080.
[25] D. Cai, H. Nie, R. Yan, J.T. Guo, T.M. Block, H. Guo, A Southern blot assay for detection of hepatitis B virus covalently closed circular DNA from cell cultures, Methods Mol. Biol. 1030 (2013) 151–161.
[26] H. Guo, C.E. Aldrich, J. Saputelli, C. Xu, W.S. Mason, The insertion domain of the duck hepatitis B virus core protein plays a role in nucleocapsid assembly, Virology 353 (2006) 443–450.
[27] H. Guo, R. Mao, T.M. Block, J.T. Guo, Production and function of the cytoplasmic deproteinized relaxed circular DNA of hepadnaviruses, J. Virol. 84 (1) (2010) 387–396.
[28] B. Hirt, Selective extraction of polyoma DNA from infected mouse cell cultures, J. Mol. Biol. 26 (2) (1967) 365–369.
[29] R.J. Lenhoff, J. Summers, Coordinate regulation of replication and virus assembly by the large envelope protein of an avian hepadnavirus, J. Virol. 68 (7) (1994) 4565–4571.
[30] K. Watashi, G. Liang, M. Iwamoto, H. Marusawa, N. Uchida, T. Daito, K. Kitamura, M. Muramatsu, H. Ohashi, T. Kiyohara, R. Suzuki, J. Li, S. Tong, Y. Tanaka, K. Murata, H. Aizaki, T. Wakita, Interleukin-1 and tumor necrosis factor-α trigger restriction of hepatitis B virus infection via a cytidine deaminase activation-induced cytidine deaminase (AID), J. Biol. Chem. 288 (44) (2013) 31715–31727.
[31] K. Watashi, A. Sluder, T. Daito, S. Matsunaga, A. Ryo, S. Nagamori, M. Iwamoto, S. Nakajima, S. Tsukuda, K. Borroto-Esoda, M. Sugiyama, Y. Tanaka, Y. Kanai, H. Kusuhara, M. Mizokami, T. Wakita, Cyclosporin A and its analogs inhibit hepatitis B virus entry into cultured hepatocytes through targeting a membrane transporter NTCP, Hepatology 59 (5) (2014) 1726–1737.
[32] A. Laras, J. Koskinas, E. Dimou, A. Kostamena, S.J. Hadziyannis, Intrahepatic levels and replicative activity of covalently closed circular hepatitis B virus DNA in chronically infected patients, Hepatology 44 (3) (2006) 694–702.
[33] M. Maynard, P. Parvaz, S. Durantel, M. Chevallier, P. Chevallier, M. Lot, C. Trepo, F. Zoulim, Sustained HBs seroconversion during lamivudine and adefovir dipivoxil combination therapy for lamivudine failure, J. Hepatol. 42 (2) (2005) 279–281.
[34] B. Werle-Lapostolle, S. Bowden, S. Locarnini, K. Wursthorn, J. Petersen, G. Lau, C. Trepo, P. Marcellin, Z. Goodman, W.E.T. Delaney, S. Xiong, C.L. Brosgart, S.S. Chen, C.S. Gibbs, F. Zoulim, Persistence of cccDNA during the natural history of chronic hepatitis B and decline during adefovir dipivoxil therapy, Gastroenterology 126 (7) (2004) 1750–1758.
[35] D.K. Wong, M.F. Yuen, H. Yuan, S.S. Sum, C.K. Hui, J. Hall, C.L. Lai, Quantitation of covalently closed circular hepatitis B virus DNA in chronic hepatitis B patients, Hepatology 40 (3) (2004) 727–737.
[36] C. Niu, H. Bao, T. Tolstykh, H.M. Micolochick Steuer, E. Murakami, B. Korba, P.A. Furman, Evaluation of the in vitro anti-HBV activity of clevudine in combination with other nucleoside/nucleotide inhibitors, Antivir. Ther. 15 (3) (2010) 401–412.
[37] D. Cai, C. Mills, W. Yu, R. Yan, C.E. Aldrich, J.R. Saputelli, W.S. Mason, X. Xu, J.T. Guo, T.M. Block, A. Cuconati, H. Guo, Identification of disubstituted sulfonamide compounds as specific inhibitors of hepatitis B virus covalently closed circular DNA formation, Antimicrob. Agents Chemother. 56 (8) (2012) 4277–4288.
[38] J. Price, An update on hepatitis B, d, and e viruses, Top. Antivir. Med. 21 (5) (2013) 157–163.
[39] Z.J. Gong, S. De Meyer, C. Clarysse, C. Verslype, J. Neyts, E. De Clercq, S.H. Yap, Mycophenolic acid, an immunosuppressive agent, inhibits HBV replication in vitro, J. Viral Hepat. 6 (3) (1999) 229–236.

Article

Immunity

The RNA Sensor RIG-I Dually Functions as an Innate Sensor and Direct Antiviral Factor for Hepatitis B Virus

Graphical Abstract

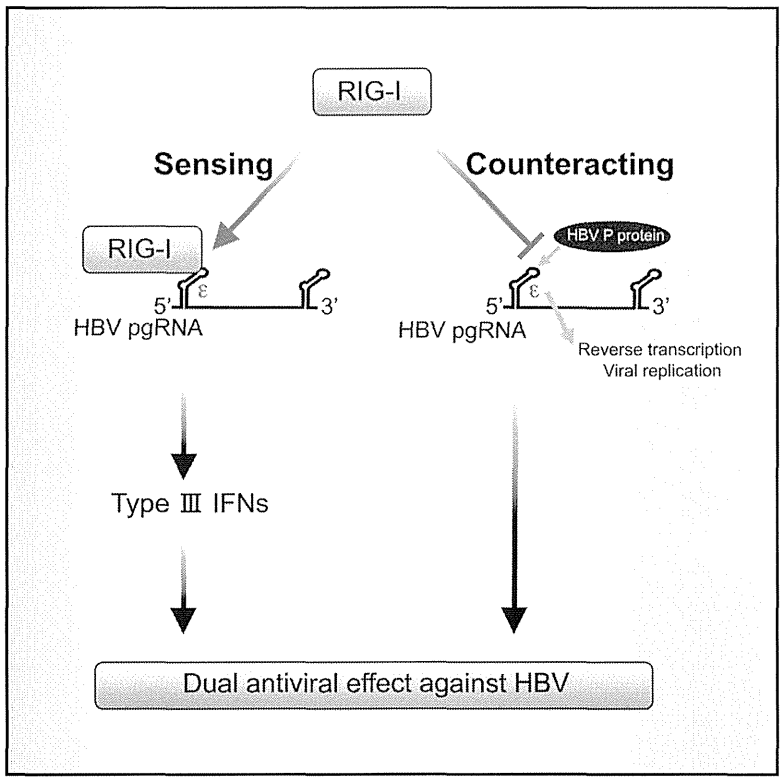

Authors

Seiichi Sato, Kai Li, ..., Yasuhito Tanaka, Akinori Takaoka

Correspondence

takaoka@igm.hokudai.ac.jp

In Brief

The sensing mechanism of hepatitis B virus (HBV) and the subsequent signaling events remain to be fully clarified. Sato and colleagues demonstrate that the RNA sensor RIG-I not only senses HBV pregenomic RNA to preferentially induce type III interferon production but also counteracts the interaction of viral polymerase with the pregenomic RNA for antiviral defense against HBV.

Highlights

- Type III IFNs are predominantly induced in human hepatocytes during HBV infection
- RIG-I senses the HBV genotype A, B, and C for the induction of type III IFNs
- The 5′-ε region of HBV pgRNA is a key element for the RIG-I-mediated recognition
- RIG-I counteracts the interaction of HBV P with pgRNA to suppress viral replication

Sato et al., 2015, Immunity *42*, 123–132
January 20, 2015 ©2015 Elsevier Inc.
http://dx.doi.org/10.1016/j.immuni.2014.12.016

CrossMark

CellPress

Immunity
Article

CellPress

The RNA Sensor RIG-I Dually Functions as an Innate Sensor and Direct Antiviral Factor for Hepatitis B Virus

Seiichi Sato,[1,2,10] Kai Li,[1,2,10] Takeshi Kameyama,[1,2,10] Takaya Hayashi,[3,10] Yuji Ishida,[4] Shuko Murakami,[5] Tsunamasa Watanabe,[5] Sayuki Iijima,[5] Yu Sakurai,[6] Koichi Watashi,[7] Susumu Tsutsumi,[5] Yusuke Sato,[6] Hidetaka Akita,[6] Takaji Wakita,[7] Charles M. Rice,[8] Hideyoshi Harashima,[6] Michinori Kohara,[9] Yasuhito Tanaka,[5] and Akinori Takaoka[1,2,*]
[1]Division of Signaling in Cancer and Immunology, Institute for Genetic Medicine, Hokkaido University, Sapporo, Hokkaido 060-0815, Japan
[2]Molecular Medical Biochemistry Unit, Biological Chemistry and Engineering Course, Graduate School of Chemical Sciences and Engineering, Hokkaido University, Sapporo, Hokkaido 060-0815, Japan
[3]Research Center for Infection-Associated Cancer, Institute for Genetic Medicine, Hokkaido University, Sapporo, Hokkaido 060-0815, Japan
[4]PhoenixBio Co., Ltd., Higashihiroshima, Hiroshima 739-0046, Japan
[5]Department of Virology and Liver Unit, Nagoya City University Graduate School of Medical Sciences, Nagoya, Aichi 467-8601, Japan
[6]Laboratory of Innovative Nanomedicine, Faculty of Pharmaceutical Sciences, Hokkaido University, Sapporo, Hokkaido 060-0812, Japan
[7]Department of Virology II, National Institute of Infectious Diseases, Tokyo 208-0011, Japan
[8]Laboratory of Virology and Infectious Disease, The Rockefeller University, New York, NY 10065, USA
[9]Department of Microbiology and Cell Biology, Tokyo Metropolitan Institute of Medical Science, Setagaya-ku, Tokyo 156-8506, Japan
[10]Co-first author
*Correspondence: takaoka@igm.hokudai.ac.jp
http://dx.doi.org/10.1016/j.immuni.2014.12.016

SUMMARY

Host innate recognition triggers key immune responses for viral elimination. The sensing mechanism of hepatitis B virus (HBV), a DNA virus, and the subsequent downstream signaling events remain to be fully clarified. Here we found that type III but not type I interferons are predominantly induced in human primary hepatocytes in response to HBV infection, through retinoic acid-inducible gene-I (RIG-I)-mediated sensing of the 5′-ε region of HBV pregenomic RNA. In addition, RIG-I could also counteract the interaction of HBV polymerase (P protein) with the 5′-ε region in an RNA-binding dependent manner, which consistently suppressed viral replication. Liposome-mediated delivery and vector-based expression of this ε region-derived RNA in liver abolished the HBV replication in human hepatocyte-chimeric mice. These findings identify an innate-recognition mechanism by which RIG-I dually functions as an HBV sensor activating innate signaling and to counteract viral polymerase in human hepatocytes.

INTRODUCTION

Hepatitis B virus (HBV) is a hepatotropic virus of the *Hepadnaviridae* family and contains a circular, partially double-stranded DNA genome of about 3.2 k base pairs that is replicated via reverse transcription of a pregenomic RNA (pgRNA). HBV causes hepatic inflammation associated with substantial morbidity worldwide (Rehermann and Nascimbeni, 2005; Protzer et al., 2012; Revill and Yuan, 2013). Around four hundred million people worldwide are persistently infected with HBV, which is a major causative factor associated with not only inflammation but also cirrhosis and even cancer of the liver. Currently, interferon (IFN) and nucleoside/nucleotide analogs are available for HBV treatment (Rehermann and Nascimbeni, 2005; Halegoua-De Marzio and Hann, 2014). However, the long-term response rates are still not satisfactory. Elucidation of host immune response against HBV infection is crucial for better understanding of the pathological processes and viral elimination to control HBV infection.

The type I IFNs, IFN-α and IFN-β, are representative cytokines that elicit host innate immune responses against viral infections. In addition, another IFN family, type III IFNs (IFN-λ, also known as IL-28 and IL-29) exhibits potent antiviral activity similar to IFN-α and IFN-β (Sheppard et al., 2003; Kotenko, 2011; Kotenko et al., 2003). Production of type I and type III IFNs is massively induced in many types of cells upon infection with various viruses, which is known to be mediated by the activation of pattern-recognition receptors (PRRs). During virus infection, virus-derived nucleic acids (both RNA and DNA) are mainly sensed by certain PRRs, such as retinoic acid-inducible gene-I (RIG-I) (Yoneyama et al., 2004; Choi et al., 2009; Chiu et al., 2009; Ablasser et al., 2009), melanoma differentiation-associated gene 5 (MDA5) (Yoneyama et al., 2005), cyclic GMP-AMP synthase (cGAS) (Sun et al., 2013), and IFN-γ-inducible protein 16 (IFI16) (Unterholzner et al., 2010). Particularly, RIG-I is a key PRR that can detect virus-derived RNAs in the cytoplasm during infection with a variety of viruses, such as influenza virus, hepatitis C virus (HCV), and measles virus, which are closely related to human disease pathogenesis (Rehwinkel and Reis e Sousa, 2010). Binding of RIG-I to its ligand RNAs, such as 5′-triphosphorylated RNA or short double-stranded RNAs (Takeuchi and Akira, 2009; Hornung et al., 2006), activates the downstream signaling pathways in a manner dependent on the adaptor protein mitochondrial antiviral

signaling protein (MAVS; also known as IPS-1, VISA, or Cardif) (Takeuchi and Akira, 2009), leading to the induction of the IFN-regulatory factor-3 (IRF-3) and NF-κB-dependent gene expression and the subsequent production of type I and type III IFNs and inflammatory cytokines (Takeuchi and Akira, 2009). Thus, RIG-I sensing of viral RNA is a crucial process to activate the antiviral innate responses to limit viral replication and the activation of adaptive immunity (Takeuchi and Akira, 2009).

As for the viruses that are known to be the leading cause of hepatic inflammation, RIG-I is the major PRR that initiates innate immune responses against HCV. RIG-I sensing of HCV is mediated through its recognition of the poly-U/UC motif of the HCV RNA genome 3′ nontranslated region, which leads to the activation of type I IFN response (Saito et al., 2008). On the other hand, earlier studies have shown that the innate immune activation is impaired and the induction of type I IFNs such as IFN-α or IFN-β is hardly detected in animal models of HBV infection, as compared with HCV infection (Wieland et al., 2004; Nakagawa et al., 2013). However, it is still not fully clarified how HBV is recognized by human hepatocytes and the role of type III IFNs as well.

Here we report that HBV infection predominately induces type III, but not type I, IFN gene induction, which is mediated by RIG-I through its recognition of the 5′-ε region of HBV-derived pgRNA. We also show that RIG-I can counteract the interaction of HBV polymerase (P protein) with the 5′-ε region of pgRNA in an RNA-binding dependent manner, resulting in the suppression of HBV replication. Furthermore, liposome-mediated delivery and expression of the 5′-ε region-derived RNA in liver suppressed the HBV replication in vivo in chimeric mice with humanized livers. Thus, our findings demonstrate the innate defense mechanisms based on the viral RNA-RIG-I interaction, whereby RIG-I functions not only as a HBV sensor for the activation of IFN response but also as a direct antiviral factor.

RESULTS

Type III IFNs Are Predominantly Induced in Hepatocytes during HBV Infection

To investigate the innate immune activation during HBV infection, we examined type I and type III IFN responses in human hepatocytes. Consistent with the previous reports (Wieland et al., 2004; Nakagawa et al., 2013), we hardly observed the induction of type I IFNs, IFN-α4, and IFN-β in response to transfection with plasmids carrying 1.24-fold the HBV genome of three major different genotypes, Ae (HBV-Ae), Bj (HBV-Bj), and C (HBV-C) (Figure 1A and Figure S1A available online) at least up to seven days after transfection, although the expression of HBV RNAs was detectable (Figure S1B). On the other hand, type III IFN, IFN-λ1, was induced in all of the three types of human hepatocyte cell line tested (Figures 1A and S1A). In HepG2 cells, HBV-C shows the highest IFN-λ1 response, which was also confirmed by ELISA, albeit weakly (Figures 1A and 1B). Moreover, IFN-λ1 in culture supernatant could inhibit vesicular stomatitis virus (VSV) replication in plaque reduction assay, as well as HBV replication (Figure S1C), indicating the physiological relevance of the induced IFN-λ1 to antiviral activities. Consistent with these results, we observed the significant induction of not only IFN-λ1 but also IFN-λ2 and -λ3 in primary human hepatocytes (PHH) in vitro 24 hr after infection with HBV-C (Figure 1C); however, neither of type I nor type II IFN tested was induced (Figures S1D and S1E). Although it is difficult to simply compare the amount of IFN induced by different types of virus, the induction of IFN-λ1, λ2, and λ3 mRNAs in response to HBV infection was much weaker than that of Newcastle disease virus (NDV) infection (Figure 1C). In this regard, in order to rule out the possibility that the IFN-λ response is due to contaminants in the inocula, we used Lamivudine (LAM), an HBV inhibitor, in this assay. Treatment with LAM inhibited IFN-λ mRNA induction in response to HBV infection in PHH (Figure 1C), suggesting that the IFN response is actually induced by HBV replication. Furthermore, we analyzed HepG2-sodium taurocholate cotransporting polypeptide (NTCP)-C4 cell line (Iwamoto et al., 2014) stably expressing human NTCP, a functional receptor for HBV (Yan et al., 2012), and confirmed that IFN-λ1 and IFN-inducible genes such as *OAS2* and *RSAD2*, but not IFN-β, were induced in these cells after infection with HBV-C, and that these inductions were abolished by treatment with LAM (Figure 1D). To next assess the innate immune responses in vivo during HBV infection, we exploited severe combined immunodeficiency mice that carry the urokinase-type plasminogen activator transgene controlled by an albumin promoter ($uPA^{+/+}$/SCID mice), in which more than 70% of murine hepatocytes were replaced by human hepatocytes (Tateno et al., 2004) (hereinafter referred to as chimeric mice). After the chimeric mice were intravenously infected with HBV-C, which was derived from patients with chronic hepatitis, the expression of type III IFN mRNAs increased in the liver tissue, whereas IFN-α4 and IFN-β mRNAs were not upregulated (Figure 1E). In parallel with this type III IFN response, we also observed the expression of IFN-inducible genes, such as *CXCL10*, *OAS2*, and *RSAD2*, in the human liver of these infected mice (Figure 1E). These findings indicate that a moderate type III but not type I or type II IFN response is activated in human hepatocytes in response to HBV infection.

HBV-Induced Type III IFN Expression Depends on RIG-I

We next determined which sensor-mediated signaling pathway is responsible for the HBV-induced type III IFN response. As HBV is a DNA virus (Rehermann and Nascimbeni, 2005; Protzer et al., 2012; Revill and Yuan, 2013), we assessed the contribution of previously reported cytosolic DNA sensors including RIG-I (Chiu et al., 2009; Ablasser et al., 2009; Choi et al., 2009), IFI16 (Unterholzner et al., 2010), and cGAS (Sun et al., 2013) in human hepatocytes. Knockdown analyses revealed that IFN-λ1 induction in HepG2 or Huh-7 cells by plasmid transfection for HBV-C or HBV-Ae, respectively, was suppressed by the knockdown of RIG-I, but not that of the other sensors (Figures 2A, S2A and S2B). To further confirm the involvement of RIG-I in HBV-triggered type III IFN response, we measured IFN-λ1 mRNA expression induced by plasmid expression in Huh-7.5 cells that carry a dominant-negative mutant RIG-I allele that prevents RIG-I signaling (Saito et al., 2007), as compared with Huh-7 cells that have an intact RIG-I pathway. Huh-7.5 cells failed to induce IFN-λ1 mRNA expression in response to HBV-Ae genome plasmid transfection, as in the case of stimulation with 5′-triphosphate RNA (3pRNA), a RIG-I ligand (Takeuchi and Akira, 2009; Hornung et al., 2006) (Figure 2B). In concordance with this result, knockdown of tripartite motif containing protein

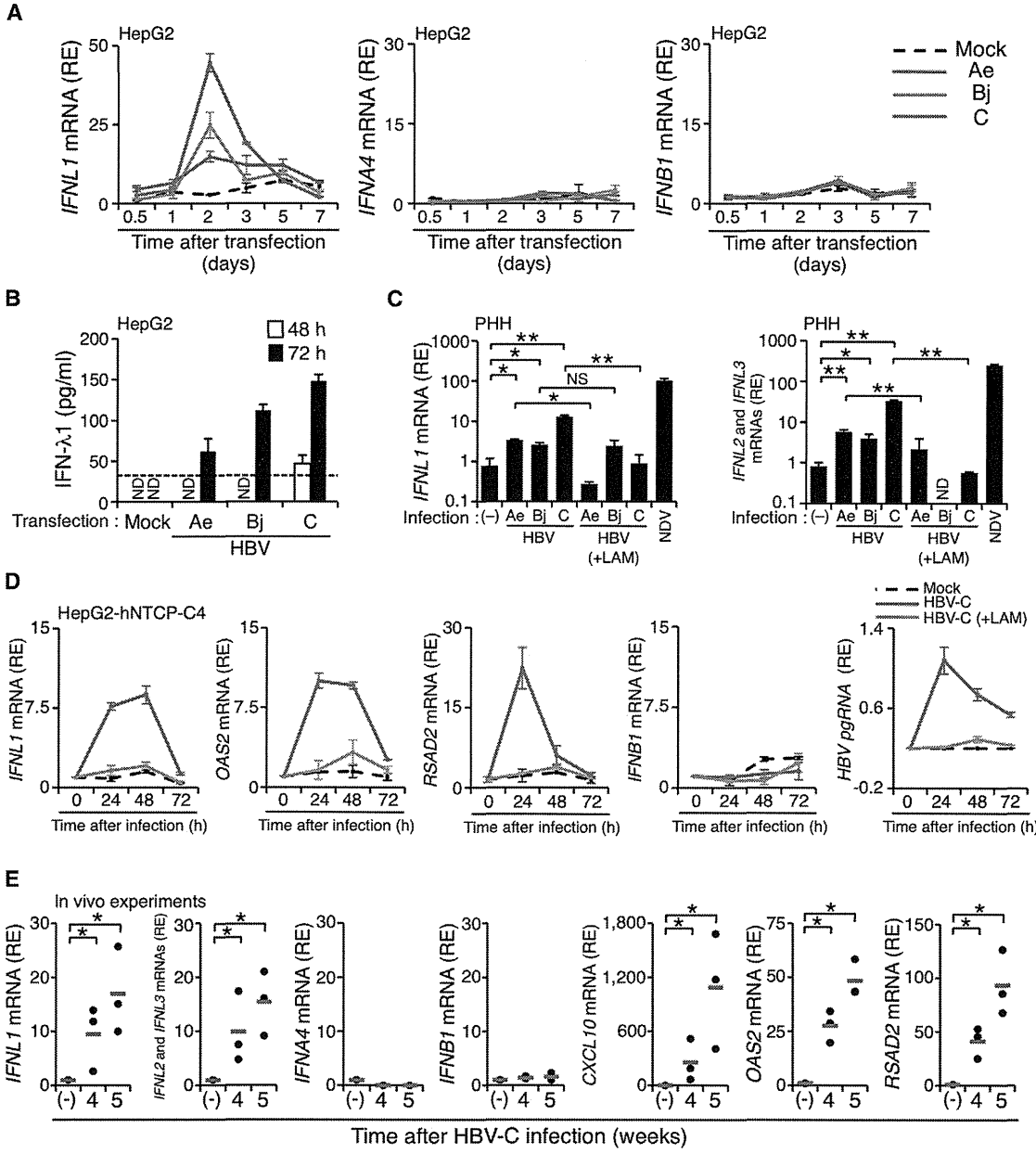

Figure 1. IFN-λ Induction in Human Hepatocytes in Response to HBV Infection

(A) Quantitative RT-PCR (qRT-PCR) analysis of *IFNL1* (left), *IFNA4* (middle), and *IFNB1* (right) mRNA at the indicated times after transfection with 1.24-fold the HBV genome (genotype Ae, Bj, or C) or empty vector (Mock) in HepG2 cells.

(B) ELISA of IFN-λ1 at 48 or 72 hr after transfection with the HBV genome in HepG2 cells. The dot line indicates the minimum detectable amount (31.2 pg/ml) of IFN-λ1 by the ELISA kit. ND, not detected, indicates below the minimum detectable amount.

(C) qRT-PCR analysis of *IFNL1*, *IFNL2*, and *IFNL3* mRNA at 24 hr after infection with HBV, NDV (multiplicity of infection = 10) or mock (–), or media-treated Lamivudine (LAM) as control in primary human hepatocytes (PHH). The mRNA copy number (±SD) of each subtype of type III IFN per 1 μg total RNA upon HBV-C infection is as follows: *IFNL1* (83,197.6 ± 6,241.4) and *IFNL2/3* (409,280.6 ± 119,676.2).

(D) Time course analyses by qRT-PCR of *IFNL1*, *OAS2*, *RSAD2*, *IFNB1* mRNA, and *pgRNA* at the indicated times after HBV infection in HepG2-hNTCP-C4 cells. The effect of Lamivudine treatment was also analyzed.

(E) qRT-PCR analysis of *IFNL1*, *IFNL2*, *IFNL3*, *IFNA4*, *IFNB1*, *CXCL10*, *OAS2*, and *RSAD2* mRNA of liver tissues at 4 or 5 weeks after infection with HBV-C in chimeric mice. (–), uninfected mice. Red lines represent the mean of each dataset. *$p < 0.05$ and **$p < 0.01$ versus control. RE, relative expression. (A–D) Data are presented as mean and SD (n = 3) and are representative of at least three independent experiments. See also Figure S1.

25 (TRIM25), MAVS, TANK-binding kinase 1 (TBK1), and IRF-3, all of which are signaling molecules essentially involved in the RIG-I-mediated IFN pathway (Takeuchi and Akira, 2009), resulted in the suppression of IFN-λ1 mRNA induction in HepG2 cells in response to transfection with the HBV-C genome. On the other hand, such an effect was not observed in cells treated

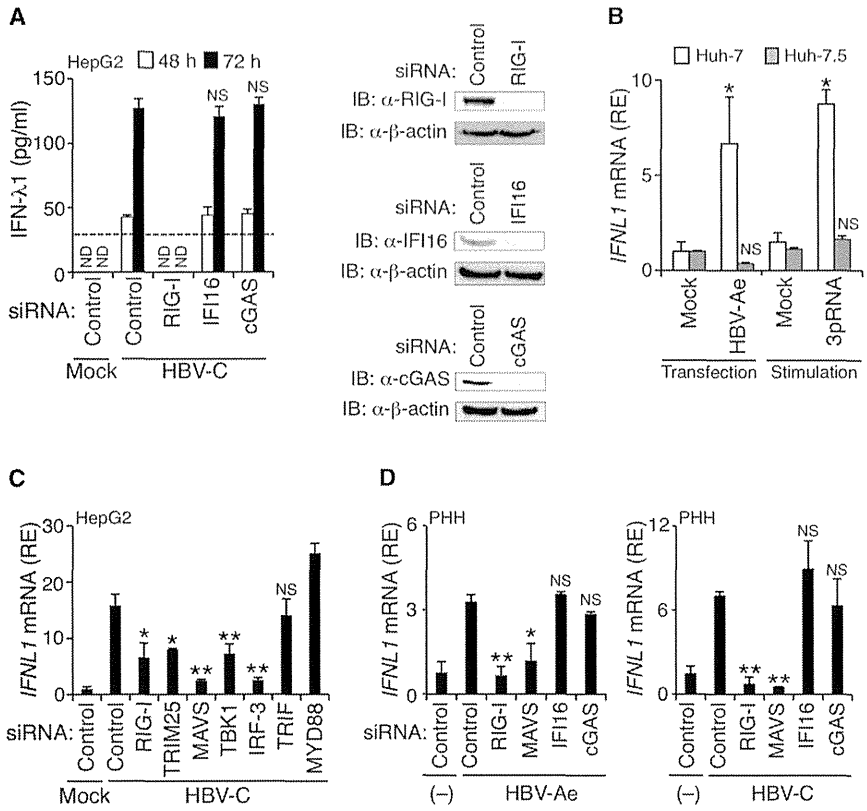

Figure 2. RIG-I-Dependent IFN-λ Induction in Response to HBV Infection

(A) HepG2 cells treated with control siRNA (Control) or siRNA targeting RIG-I, IFI16, or cGAS were transfected with the HBV-C genome for 48 or 72 hr. The amount of IFN-λ1 were measured by ELISA. The dot line indicates the minimum cytokine expression detected (31.2 pg/ml) of IFN-λ1 by the ELISA kit. ND, not detected, indicates below detectable concentrations (left), and knockdown efficiency was analyzed by immunoblotting (IB) (right).

(B) qRT-PCR analysis of *IFNL1* mRNA in Huh-7 or Huh-7.5 cells transfected with the HBV-Ae genome (at 24 hr after transfection) or stimulated with 3pRNA (1 μg/ml) for 6 hr.

(C) HepG2 cells treated with control siRNA (Control) or the indicated siRNAs were transfected with the HBV-C genome. At 48 hr after transfection, total RNAs were subjected to qRT-PCR analysis for *IFNL1*.

(D) qRT-PCR analysis of *IFNL1* mRNA in siRNA-treated PHH at 24 hr postinfection with indicated HBV genotype. Mock, empty vector-transfected. (–), uninfected. Data were normalized to the expression of *GAPDH*. Data are presented as mean and SD (n = 3) and are representative of at least three independent experiments. *p < 0.05 and **p < 0.01 versus control in (B) or HBV-infected control group in (A, C, and D). NS, not significant. See also Figure S2.

with either TRIF (also known as TICAM-1) or MYD88 siRNA (Figures 2C and S2C). In addition, we confirmed that the knockdown of RIG-I and MAVS abolished IFN-λ1 induction in PHH infected with each genotype (Figure 2D). Furthermore, we also confirmed by knockdown assay that the induction of IFN-λ1 and OAS2 mRNA in HepG2-hNTCP-C4 cells in response to infection with HBV-C was dependent on RIG-I (Figure S2E). These data indicate that IFN-λ1 gene induction during HBV infection depends largely on RIG-I signaling pathway.

The 5′-ε Region of HBV pgRNA Is a Key Element for RIG-I-Dependent IFN-λ1 Induction

RIG-I can recognize not only virus-derived RNA but also DNA in the cytoplasm (Yoneyama et al., 2004; Choi et al., 2009; Chiu et al., 2009; Ablasser et al., 2009). To further clarify how RIG-I recognizes HBV, we first examined either or both of which nucleic acid (DNA and RNA) derived from HBV-infected cells can activate IFN-λ1 gene expression. Transfection with nucleic acid fractions extracted from HBV infected Huh-7 cells after pretreatment with RNase A, but not DNase I resulted in marked inhibition of the *IFNL1* promoter activation, suggesting that virus-derived RNAs might be candidates of the RIG-I ligand during HBV infection (Figure 3A).

The HBV genome comprises a partially double-stranded 3.2 kb DNA. During a life cycle of HBV in hepatocytes, its covalently closed circular DNA (cccDNA) is transcribed to generate four major RNA species: the 3.5, 2.4, 2.1, and 0.7 kb viral RNA transcripts (Rehermann and Nascimbeni, 2005; Protzer et al., 2012; Revill and Yuan, 2013). We created an siRNA to suppress the expression of all of these RNA transcripts and tested its effect on HBV-induced IFN-λ1 expression. As shown in Figure 3B, knockdown with this siRNA (Figure S3A) suppressed IFN-λ1 induction in Huh-7 cells transfected with HBV-Ae. Next, to determine which of these HBV RNA transcripts is/are involved in the RIG-I-mediated IFN-λ1 induction, we prepared expression vectors to express each of these four viral transcripts in HEK293T cells that are often used to analyze RIG-I signaling pathway in human cells. As a result, it is only the longest 3.5 kb transcript, that is, pgRNA, that has the potential to elicit a significant induction of IFN-λ1 mRNA (Figures 3C and S3B). It was also confirmed by knockdown analysis with pgRNA-targeted siRNA, which showed significant suppression of IFN-λ1 induction in HepG2 cells transfected with HBV-Ae (Figure S3C). These results suggest that 5′-1.1 kb region of HBV pgRNA is critical for the activation of RIG-I pathway to induce IFN-λ1 expression. On the other hand, the remaining three transcripts, which also contain the same sequence of part of this 1.1 kb region of HBV pgRNA at the 3′ end of their transcripts, failed to induce IFN-λ1 mRNA (Figure 3C). An artificially deleted form of pgRNA, which lacks this overlapping sequence at the 3′-region (Δ3), showed IFN-λ1 induction, whereas such response was not observed for another mutant pgRNA lacking it at the 5′-region (Δ5) (Figure 3D). These data also support a possible important role of the 5′-overlapping sequence of HBV pgRNA for RIG-I-mediated IFN-λ1 induction.

The 5′-end of HBV pgRNA is known to contain the encapsidation sequence, called "epsilon (ε)," which takes a stem-loop secondary structure (Junker-Niepmann et al., 1990; Pollack and

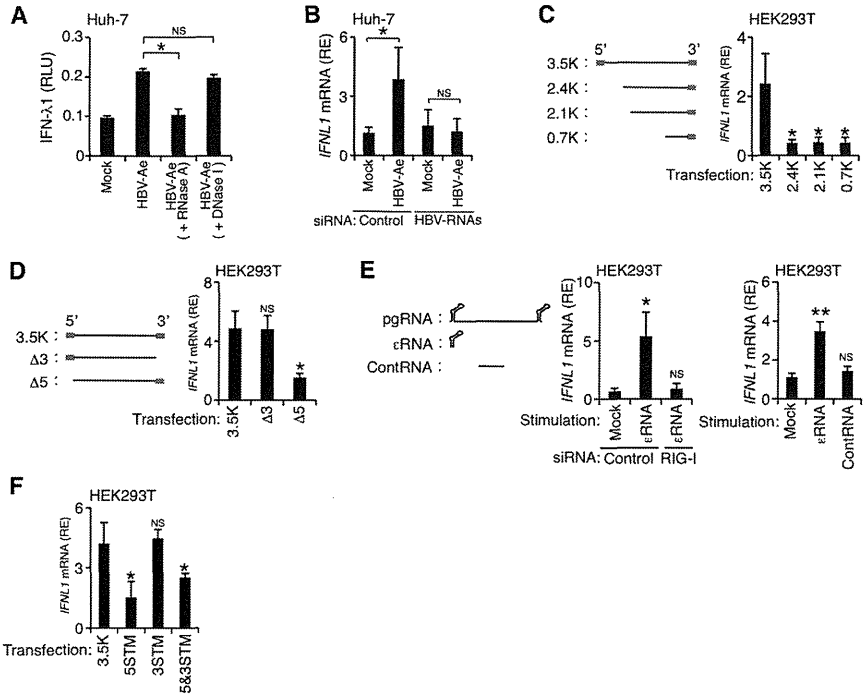

Figure 3. RIG-I Activation Is Mediated by Its Recognition of the 5′-ε Region of HBV pgRNA

(A) Luciferase activity of an IFN-λ1 reporter plasmid after 24 hr of stimulation with nucleic acids (2 μg/ml) extracted from Huh-7 cells transfected with control plasmid (Mock) or the HBV-Ae genome with or without RNase A or DNase I treatment. RLU, relative luciferase units.

(B) Huh-7 cells treated with control or HBV RNA-targeted siRNA were transfected with the HBV-Ae genome or mock. After 24 hr of transfection, total RNAs were subjected to qRT-PCR for *IFNL1*.

(C and D) A schematic representation of four types of HBV RNAs, pgRNA (3.5 kb), 2.4 kb, 2.1 kb, and 0.7 kb RNAs in (C), and two deleted forms of pgRNA, Δ5 and Δ3, in (D). The overlapping region is shown in blue. qRT-PCR analysis of *IFNL1* mRNA of HEK293T cells after 24 hr of transfection with the indicated expression vectors. Data were normalized to the amount of each HBV RNA expression (C and D).

(E) A schematic representation of pgRNA, εRNA, or control RNA (ContRNA) (left). HEK293T cells treated with control or RIG-I siRNA were unstimulated (Mock) or stimulated with εRNA for 12 hr. Total RNAs were subjected to qRT-PCR for *IFNL1* (middle). qRT-PCR analysis of *IFNL1* mRNA in HEK293T cells after 12 hr of stimulation with εRNA or ContRNA (right). Each of the RNAs was prepared by in vitro transcription.

(F) HEK293T cells were transfected with each plasmid for stem-loop mutants of pgRNA (5STM, 3STM, or 5 and 3STM), and then subjected to qRT-PCR analysis as described in (C). *$p < 0.05$ and **$p < 0.01$ versus control in (A, B, and E) or versus 3.5K in (C, D, and F). NS, not significant. See also Figure S3.

Ganem, 1993; Knaus and Nassal, 1993; Jeong et al., 2000). Therefore, we hypothesized that this 5′-ε structure might confer a possible pathogen-associated molecular pattern (PAMP) motif for RIG-I recognition. To test this hypothesis, we stimulated HEK293T and HepG2 cells with the ε region-derived RNA (hereafter called εRNA). Consequently, IFN-λ1 mRNA was significantly induced, which was dependent on RIG-I, while such a response was not detected upon stimulation with the equivalent length of RNA that is derived from HBV pgRNA but does not contain any ε element (ContRNA) (Figure 3E and S3D). We also confirmed RIG-I-dependent IRF-3 activation in response to stimulation with εRNA (Figures S3D and S3E). Due to the overlapping sequence of 5′- and 3′-ends of HBV pgRNA as mentioned above, this ε element is found at both ends of pgRNA. We next generated several mutant forms of HBV pgRNA, each of which carries mutations within 5′- or 3′-ε region or both to disrupt the stem-loop structure (5STM, 3STM, or 5 and 3STM, respectively). In concordance with the results shown in Figures 3C and 3D and S3B, IFN-λ1 mRNA induction was detected upon expression of the 3STM transcript that has an intact 5′-ε region, as similar to that of intact 3.5-kb pgRNA (Figure 3F). In contrast, either 5STM or 5 and 3STM did not show significant response. These findings indicate that the 5′-ε region of HBV pgRNA is critical for IFN-λ1 induction possibly through the recognition by RIG-I.

RIG-I Interacts with the ε-Region of pgRNA

Next, we assessed the interaction of RIG-I with the ε region of HBV pgRNA, that is, εRNA. Pull-down assays showed that Flag-tagged RIG-I was coprecipitated with εRNA, but not with ContRNA, in HEK293T cells (Figure 4A, top). Similarly, endogenous RIG-I interacted with εRNA albeit weakly (Figure 4A, bottom). We also demonstrated the intracellular colocalization of RIG-I with εRNA in Huh-7.5 cells (Figure 4B). In addition, RNA-binding protein immunoprecipitation (RIP) assay revealed that the full length of HBV pgRNA was detected in the RIG-I-immunoprecipitated complex, and Δ5 pgRNA and Δ3 pgRNA were also detected (Figure S4A), which is seemingly inconsistent with the results by the functional assay (Figures 3C, 3D, 3F and S3C). These results suggest that the ε region is required for its interaction with RIG-I, but only the 5′-ε region is necessary to activate RIG-I pathway. We further tried to determine which region of RIG-I mediates its interaction with HBV pgRNA. Both RIP assay and RNA pull-down assay with several deletion mutants of RIG-I showed that the C-terminal portion of RIG-I (C-RIG) including its helicase domain and repressor domain (RD) except for CARDs can bind to HBV pgRNA (Figure 4C; Figures S4B and S4C). In addition, gel shift assay showed that the interaction of HBV εRNA or pgRNA was impaired with the RD or C-RIG mutant, respectively, each of which carries a point mutation (K888E) that abolishes its RNA-binding activity (Cui et al., 2008) (Figure 4D). A similar result was also obtained by RIP assay, wherein the wild-type (WT) C-RIG, but not the K888E mutant, was coimmunoprecipitated with HBV pgRNA (Figure S4D), like HCV RNA that was previously reported to interact with RIG-I (Figure S4E). We also confirmed the interaction of HBV pgRNA with endogenous RIG-I in HepG2 cells, whereas its interaction with other nucleic acid sensors, such as IFI16 and MDA5 (Yoneyama et al., 2005), was not detected (Figure 4E). These data indicate that

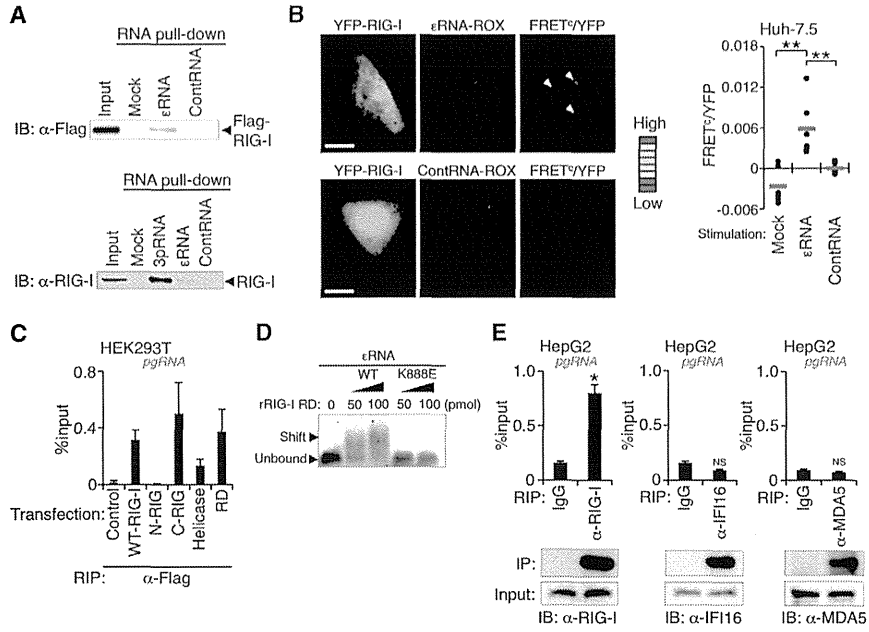

Figure 4. RIG-I Interacts with the ε Region of pgRNA

(A) RNA pull-down assay showing the binding activity of the indicated RNAs to Flag-tagged RIG-I (Flag-RIG-I) in HEK293T cells (top) or endogenous RIG-I in HepG2 cells (bottom).

(B) FRET analysis for the interaction of YFP-tagged RIG-I (YFP-RIG-I) with rhodamine (ROX)-conjugated εRNA (εRNA-ROX) or ContRNA (ContRNA-ROX). Representative fluorescence images of YFP, ROX, and FRET^C/YFP (the ratio of corrected FRET (FRET^C) to YFP). *Arrowheads* indicate area showing high FRET efficiency. Scale bar represents 20 μm. Right, dot plot of FRET^C/YFP ratio (small horizontal bars, mean).

(C) RIP assay with HEK293T cell lysates expressing several Flag-tagged deletion mutants of RIG-I and pgRNA expression vector by using anti-Flag antibody. Immunoprecipitated pgRNA was quantitated by qRT-PCR and normalized to the amount of immunoprecipated proteins (Figure S4C) and is represented as fraction of input RNA prior to immunoprecipitation (percentage input).

(D) Gel-shift analysis of complex formation between εRNA and recombinant RIG-I RD (WT) or RD (K888E). Arrowheads denote position of unbound RNA and RNA–RIG-I complexes.

(E) RIP assay with HepG2 cell lysates prepared after 48 hr of transfection of the HBV-C genome by using anti-RIG-I, anti-IFI16, anti-MDA5, or control immunoglobulin G. The immunoprecipitated pgRNA was measured by qRT-PCR (top) as described in (C). Whole-cell expression and immunoprecipitated amounts of RIG-I, IFI16, and MDA5 (bottom). Data are presented as mean and SD (n = 3) and are representative of at least three independent experiments. *p < 0.05 and **p < 0.01 versus control in (B and E). NS, not significant. See also Figure S4.

the 5′-ε region of viral pgRNA functions as an HBV-associated molecular pattern to be specifically recognized by RIG-I and can trigger IFN-λ response.

RIG-I Exerts an Antiviral Activity by Counteracting the Interaction of HBV Polymerase with pgRNA

We next assessed the contribution of RIG-I pathway in antiviral defense against HBV infection. RIG-I knockdown in PHH resulted in a higher HBV genome copy number at 10 days after infection with HBV-C, as compared with PHH treated with control siRNA (Figure 5A). A similar observation was made for RIG-I siRNA-treated HuS-E/2 cells (Figure S5A). These results indicate an implicated role of RIG-I as an innate sensor to activate antiviral response against HBV infection. On the other hand, it has been previously reported that the 5′-ε region of HBV pgRNA is important to serve as a binding site of viral P protein for initiating reverse transcription (Bartenschlager and Schaller, 1992). As consistent with this, we showed that the P protein interacts with εRNA in Huh-7.5 and HEK293T cells, by fluorescence resonance energy transfer (FRET) analysis (Figure 5B) and RNA pull-down assay (Figure S5B), respectively. These findings facilitated us to examine whether RIG-I could block the access of P protein toward the ε region. As we expected, recombinant RIG-I protein suppressed the interaction of P protein with pgRNA in a dose-dependent manner (Figure 5C). Such an inhibitory effect was also observed in Huh-7.5 cells by expression of WT RIG-I, as well as its T55I (Sumpter et al., 2005; Saito et al., 2007) or K270A (Takahasi et al., 2008) mutant (Figures 5D and S5C), both of which are not able to induce ligand-dependent activation of the downstream signaling but retain their RNA-binding activities. On the other hand, the K888E (Cui et al., 2008) mutant could not inhibit the binding of P protein with pgRNA (Figures 5D and S5C). In addition, treatment with recombinant IFN-λ1 in Huh-7.5 cells upregulated the amount of the mutant RIG-I protein (T55I) (Figure S5D), resulting in a partial inhibition of the P protein interaction with pgRNA, and this inhibitory effect was abrogated by RIG-I knockdown (Figure 5E). In fact, FRET analysis showed that the P protein-εRNA interaction was significantly suppressed by expression of the RIG-I RD (WT) alone, but not the mutant RD (K888E) (Figure S5E). Furthermore, HBV replication was also suppressed by expression of the RIG-I RD (WT) in Huh-7.5 cells, wherein any IFN induction is not observed, while the mutant RD (K888E) did not affect viral replication (Figure 5F). These findings revealed another aspect of RIG-I as a direct antiviral factor through its interference with the binding of HBV P protein to pgRNA in an IFN pathway-independent manner.

The εRNA Restricts HBV Replication in Human Hepatocyte-Chimeric Mice

Lastly, based on the above results, we tried to harness the therapeutic potential of the P protein-interacting εRNA for the control of HBV infection. A vector was designed to include a 63 bp DNA oligo, which is transcribed into an εRNA. We confirmed in the in vitro experiments using Huh-7.5 cells that εRNA induced by this vector-driven expression is capable to function as a decoy RNA to interfere with the binding of HBV P protein to pgRNA and to inhibit viral replication in an IFN-independent manner (Figures 6A and 6B, left). On the other hand, εRNA did not show any difference in HCV replication as compared with control (Figure 6B, right). In order to evaluate the therapeutic efficacy of εRNA in vivo, we exploited HBV infection model of human

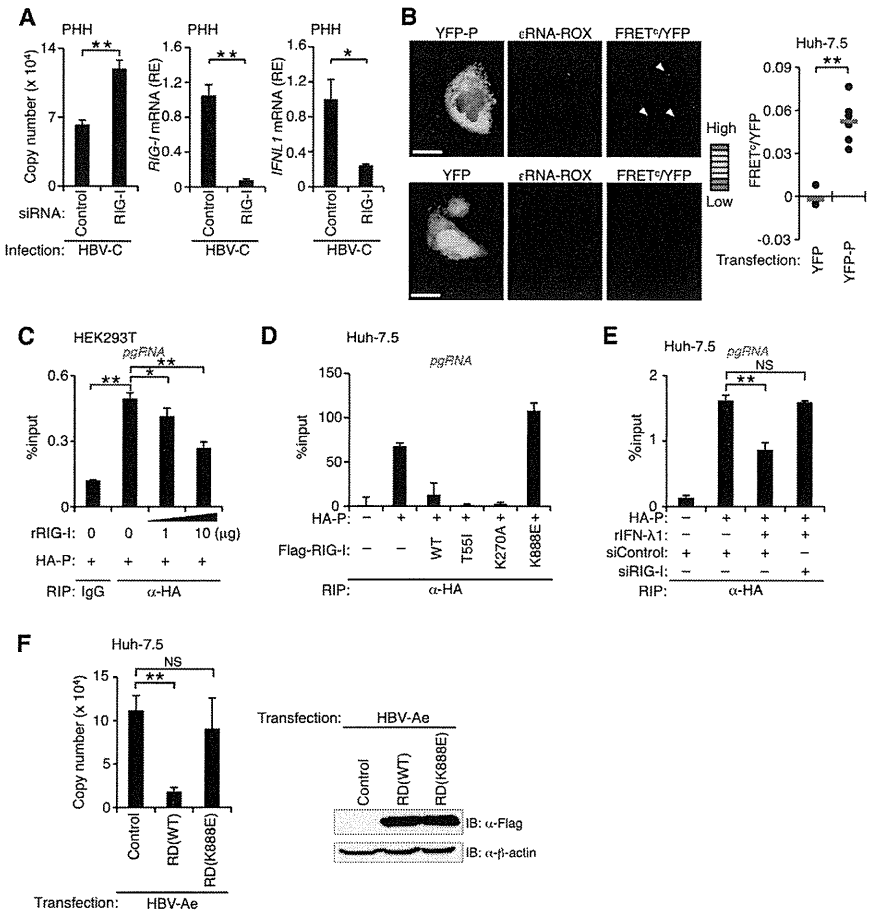

Figure 5. RIG-I Functions as an Antiviral Factor by Counteracting the Interaction of HBV P Protein with pgRNA

(A) qPCR analysis of copy numbers of encapsidated HBV DNA (left) and qRT-PCR analysis of *RIG-I* (middle) and *IFNL1* mRNA (right) in control or RIG-I siRNA-treated PHH after 10 days of infection with HBV-C.

(B) FRET analysis for the interaction between YFP-tagged P protein (YFP-P) or YFP and εRNA-ROX as described in Figure 4B. Scale bar represents 20 μm. Arrowheads indicate area showing high FRET efficiency.

(C) HEK293T cell lysates expressing pgRNA and HA-tagged P protein (HA-P) were incubated with the indicated amount of recombinant RIG-I (rRIG-I). The interaction of pgRNA with HA-P was analyzed by RIP assay and qRT-PCR analysis as described in Figure 4C.

(D) Cell lysates from Huh-7.5 cells expressing HBV pgRNA, HA-P, and Flag-RIG-I or its mutants as indicated were subjected to RIP assay for the characterization of the capability of RIG-I to counteract the interaction of pgRNA with HA-P, as described in Figure 4C.

(E) The effect of rIFN-λ1 treatment on the interaction of pgRNA with HA-P in Huh-7.5 cells was assessed by RIP assay. Huh-7.5 cells expressing both pgRNA and HA-P were treated with rIFN-λ1 (100 ng/ml) for 24 hr, and subjected to RIP assay as described in Figure 4C. RIG-I dependency was also determined by RIG-I knockdown analysis.

(F) Huh-7.5 cells were transfected with an expression vector for RIG-I RD (WT) or RD (K888E), together with the HBV-Ae genome. After 72 hr of transfection, copy numbers of encapsidated HBV DNA were measured (left), as described in (A). Expression of Flag-RIG-I RD (WT) and RD (K888E) (right). *$p < 0.05$ and **$p < 0.01$ versus control. NS, not significant. See also Figure S5.

hepatocyte-chimeric mice. HBV-infected mice underwent intravenous administration with the εRNA expression vector loaded in a liposomal carrier, a multifunctional envelope-type nanodevice (MEND) for efficient delivery, for 2 weeks. Treatment with εRNA-MEND significantly suppressed the elevation of the number of viral genome copies in the sera by less than one tenth of those for control mice (Figure 6C). Consistently, immunofluorescence analyses showed that the expression of HBV core antigen (HBcAg) in the liver tissues of εRNA-MEND-treated chimeric mice was remarkably reduced as compared with those of control mice (Figure 6D).

DISCUSSION

The innate immune system acts as a front line of host defense against viral infection. In this step, PRRs play a crucial role in the recognition of invading viruses. In particular, nucleic acid sensing of viruses is central to the initiation of antiviral immune responses. In this study, we tried to seek for a relevant nucleic acid sensor(s) for HBV and to characterize the IFN response during HBV infection. As a result, we have identified RIG-I as an important innate sensor of HBV to predominantly induce type III IFNs in hepatocytes through its recognition of the 5′-ε stem-loop of HBV pgRNA (Figures 1, 2, 3, and 4). In this respect, there have also been several reports showing that HBV X or P protein interacts with MAVS or competes for DDX3 binding with TBK1, respectively (Wei et al., 2010; Wang and Ryu, 2010; Yu et al., 2010), and inhibits RIG-I-mediated type I IFN pathway, which possibly enables HBV to evade from antiviral innate immune response. This would mirror the important role of RIG-I-mediated signaling for antiviral defense against HBV infection, although further investigation will be required to determine whether other sensing molecules except for RIG-I are engaged in the activation of innate responses in other cell types including dendritic cell subsets. Interestingly, Lu et al. have recently showed that the genotype D of HBV is sensed by MDA5, but not RIG-I, which is based only upon the analyses with HBV genome (2-fold) plasmid transfection in a single cell line Huh-7 (Lu and Liao, 2013). In this respect, we presume that such seemingly contradictory results might arise mainly from the difference in HBV genotype: It has been reported that the genotype D is phylogenetically different from the genotypes A, B, and C, which we analyzed in this study (Kato et al., 2002).

In addition, according to our results (Figure 1C and S1C), HBV-induced type III IFN response does not seem to be efficient as compared with the case with NDV infection. We speculate that

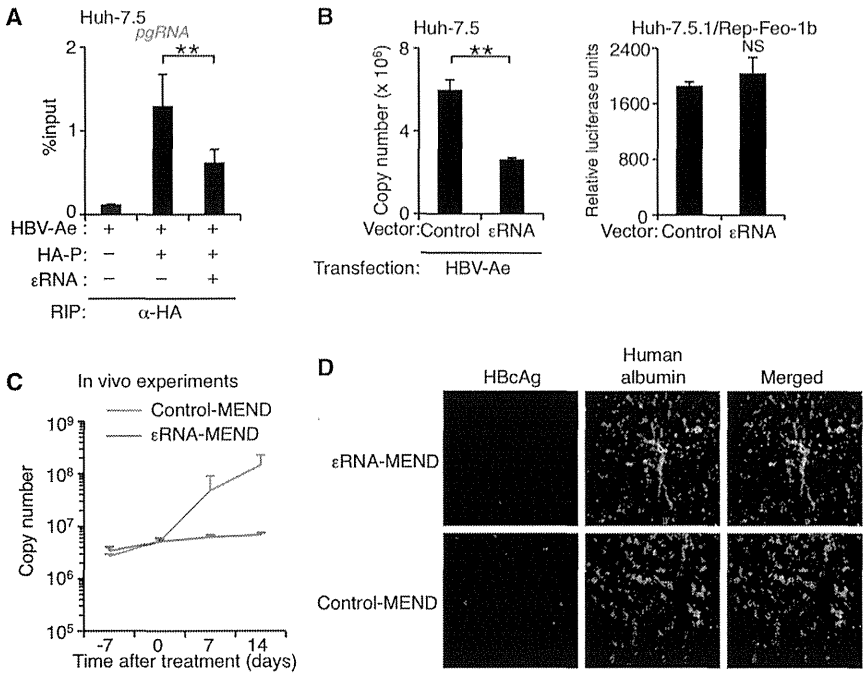

Figure 6. Inhibition of HBV Replication by εRNA

(A) Huh-7.5 cells were transfected with expression vectors for HA-P and εRNA, together with the HBV-Ae genome. RIP assay was performed to evaluate the effect of εRNA on the interaction between HA-P and pgRNA, as described in Figure 5D.

(B) Copy numbers of encapsidated HBV DNA in Huh-7.5 cells expressing the HBV-Ae genome and εRNA, as determined by qPCR (left). HCV replication in Huh-7.5.1/Rep-Feo-1b cells expressing εRNA, as determined by luciferase assay (right).

(C) HBV-infected mice were intravenously administrated with the εRNA expression vector (εRNA-MEND) or empty vector (Control-MEND) loaded in liposomal carrier at a dose of 0.5 mg/kg of body weight every 2 days for 14 days. Serum HBV DNA in HBV-infected chimeric mice was determined by qPCR (n = 3 per group). Day 0 indicates the time of the initiation of administration.

(D) Immunofluorescence imaging was performed for the detection of HBcAg (red) and human albumin (green) in the liver sections of HBV-infected chimeric mice at 14 days after treatment with εRNA-MEND or Control-MEND as described in Experimental Procedures. Data are presented as mean and SD (n = 3) and are representative of at least three independent experiments. **p < 0.01 versus control. NS, not significant.

the weakness of the IFN response during HBV infection might attribute at least in part to these viral evasions from host-cell control, which would be supported by our preliminary data showing that one HBV mutant, which generates viral RNAs including pgRNA but lacks the ability to express whole viral proteins including HBV X and P proteins, can induce higher amounts of IFN-λ1 than intact HBV (Figure S1G). In relevance with this, our present data indicate that the interaction of HBV P protein with the 5′-ε stem-loop affects the RIG-I-mediated recognition of viral pgRNA and the subsequent downstream signaling events, which might likely suppress the induction of IFN-λs. This might provide an aspect of HBV P protein in terms of viral evasion from RIG-I activation. As for the mechanism for the preferential induction of type III IFNs in hepatocytes in response to HBV, as well as HCV (Nakagawa et al., 2013; Park et al., 2012), we might speculate the existence of a hepatocyte-specific factor(s), which is selectively involved in type III IFN gene induction, although this issue merits further investigation including epigenetic evaluation of human hepatocytes. We also found that either of the 5′- or 3′-ε region of pgRNA could interact with RIG-I but it was only the 5′-ε region that contributed to the induction of IFN-λ1 (Figures 3D and S4A). In this respect, we presume that some cofactor(s) might additionally determine the preferential use of the 5′-ε region for RIG-I activation; however, it would be a next interesting issue to be solved. In addition to this, our data demonstrated a hitherto-unidentified function of RIG-I as a direct antiviral factor against HBV infection (Figure 5). Mechanistically, RIG-I was found to counteract the accessibility of HBV P protein to the 5′-ε stem-loop of pgRNA, which is an important process for the initiation of viral replication (Bartenschlager and Schaller, 1992). As is the case with this, several viral PAMPs known to be recognized by RIG-I, for example, the poly-U/UC tract in the 3′ nontranslated region of HCV genome (Saito et al., 2008) and 5′ terminal region of influenza virus genome (Baum et al., 2010) were previously reported to be directly or indirectly critical for viral replication (You and Rice, 2008; Huang et al., 2005; Moeller et al., 2012). In this respect, one could envisage that such an exquisite targeting by RIG-I would confer a unique machinery to ensure efficient antiviral activities of RIG-I. Therefore, RIG-I is likely to play dual roles as an innate sensor and as a direct antiviral effector for host defense during viral infection.

In relation to the evaluation of the experiments shown in Figures 6C and 6D, we additionally analyzed the following points: When we treated HepG2 cells with εRNA-MEND or Control-MEND, in both cases we hardly detected the massive induction of cytokines such as *TNF*, *IL6*, and *CXCL10* (data not shown). This was further confirmed by analyzing SCID mice injected with εRNA-MEND or Control-MEND (data not shown). In addition, εRNA-MEND has the specific effect on the replication of HBV, but not HCV in Huh-7.5 cells (Figure 6B). These data suggest that the results (Figures 6C and 6D) might not be mainly influenced by massive production of antiviral cytokines, although the cross-reactivity of cytokines should be still carefully considered. Therefore, it is presumed that the effect of εRNA might be based on not only its antagonistic activity but also its cytokine-inducing activity. These findings might afford a new therapeutic modality in replace of conventional antiviral drugs that have been reported to have a risk to develop drug-resistance HBV (Song et al., 2012). The present study might provide a better approach to the strategy for development of nucleic acid medicine and offer an attractive clinical option for the therapy against not only HBV but also possibly other virus infections.

EXPERIMENTAL PROCEDURES

Infection of Human Hepatocyte-Chimeric Mice with HBV and In Vivo Treatment with εRNA

To generate human hepatocyte-chimeric mice, uPA$^{+/+}$/SCID mice, were transplanted with commercially available cryopreserved human hepatocytes (a 2-year-old Hispanic female; BD Bioscience) as described previously (Tateno et al., 2004). Chimeric mice were intravenously infected with HBV-C (10^6 copies per mouse) derived from patient with chronic hepatitis (Sugiyama et al., 2006). Total RNAs were isolated from liver tissues at 0, 4, or 5 weeks after infection and subjected to quantitative RT-PCR (qRT-PCR). In preparation for εRNA treatment, HBV infection at 3 weeks after infection was confirmed by measuring the number of viral genome copies in the sera of HBV-infected chimeric mice by qPCR analysis, and at 4-week postinfection, εRNA expression vector or empty vector loaded in a liposomal carrier, a multifunctional envelope-type nanodevice (MEND), was administered intravenously at a dose of 0.5 mg/kg of body weight (n = 3 per group) every two days for 14 days. Serum samples were subjected to qPCR for the quantification of DNA copy numbers of HBV as described previously (Nakagawa et al., 2013). All animal protocols described in this study were performed in accordance with the Guide for the Care and Use of Laboratory Animals and approved by the Animal Welfare Committee of Phoenix Bio Co., Ltd.

HBV Infection in Human Hepatocytes and Quantification of Encapsidated HBV DNA

HBV infection in PHH or HepG2-hNTCP-C4 cells was performed at 10 or 100 genome equivalents per cell, respectively, in the presence of 4% PEG8000 at 37°C for 24 hr as previously described (Sugiyama et al., 2006; Watashi et al., 2013; Iwamoto et al., 2014). Lamivudine (50 μM; Sigma) was added in Huh-7 culture media during HBV production. HBV DNA was purified from intracellular core particles as described previously (Turelli et al., 2004; Fujiwara et al., 2005). Briefly, cells were suspended in lysis buffer containing 50 mM Tris-HCl (pH 7.4), 1 mM EDTA, and 1% NP-40. Nuclei were pelleted by centrifugation at 4°C and 15,000 rpm for 5 min. The supernatant was adjusted to 6 mM MgOAc and treated with DNase I (200 μg/ml) and of RNase A (100 μg/ml) for 3 hr at 37°C. The reaction was stopped by addition of 10 mM EDTA and the mixture was incubated for 15 min at 65°C. After treatment with proteinase K (200 μg/ml), 1% SDS, and 100 mM NaCl for 2 hr at 37°C, viral nucleic acids were isolated by phenol:chloroform:isoamyl alcohol (25:24:1) extraction and ethanol precipitation with 20 μg glycogen. Copy numbers of HBV DNA were measured by qPCR with the indicated primers (Table S3).

qRT-PCR Analysis

Total RNAs were isolated from culture cells or frozen liver tissue using Isogen (Nippon Gene) and were treated with DNase I (Invitrogen). cDNA was prepared from total RNAs using ReverTra Ace (TOYOBO). qRT-PCR was performed using SYBR Premix Ex Taq (TAKARA) and analyzed on a StepOnePlus real-time PCR system (Applied Biosystems). Detailed information about the primers used here is shown in Table S3. Data were normalized to the expression of *GAPDH* or HBV RNAs for each sample.

RIP Assay

After 2 hr incubation with the antibody as indicated for immunoprecipitation, cell lysates were mixed with Protein-G Dynabeads (Invitrogen) and further incubated for 1 hr with gentle shaking. After washing three times, the precipitated RNAs were analyzed by qRT-PCR with appropriate primers to detect the target RNA. The amount of immunoprecipitated RNAs is represented as the percentile of the amount of input RNA (percentage input). The detail was described in the Supplemental Experimental Procedures.

SUPPLEMENTAL INFORMATION

Supplemental Information includes five figures, four tables, and Supplemental Experimental Procedures and can be found with this article online at http://dx.doi.org/10.1016/j.immuni.2014.12.016.

AUTHOR CONTRIBUTIONS

S.S., K.L., T.K., and T.H. carried out most of the experiments and analyzed data. Y.T. provided materials of HBV and designed the protocol for infection. Y.I. conducted HBV infection in chimeric mice and preparation of human hepatocytes, and S.M., T. Watanabe, S.I., S.T., and Y.T. performed the related analysis and contributed to the interpretation of the results. C.M.R. offered critical advice on the whole manuscript and provided a pair of Huh-7 and Huh-7.5 cell lines. K.W. and T. Wakita provided HepG2-hNTCP-C4 cells. T.K. carried out FRET analysis. Y. Sakurai, Y. Sato, H.A., and H.H. syntheses of plasmid-loaded MEND, and M.K. contributed to establishment of the protocols for in vivo treatment. A.T. supervised the project, designed experiments and wrote the manuscript with critical input from the coauthors, and all authors contributed to discussing the results.

ACKNOWLEDGMENTS

We thank M. Hijikata and K. Shimotohno for HuS-E/2 cell line, N. Sakamoto for Huh-7.5.1/Rep-Feo-1b cells, J. Miyazaki for pCAGGS vector, A. Miyawaki for pCAGGS-YFP vector, T. Fujita for the luciferase reporter plasmid p-55C1BLuc, A. Takada for VSV, H. Kida for NDV, H. Ishizu and T. Hirose for technical advice on RIP assay, and A. Bergthaler, A. Shlomai, T. Saito, and M. Yasuda for critical reading of the manuscript and helpful advice. The authors are grateful for financial supports from the Ministry of Health, Labour and Welfare of Japan (Grant-in-Aid to A.T. and Y.T.), the Ministry of Education, Culture, Sports, Science and Technology of Japan (Grant-in-Aid for Scientific Research [A] [25253030] to A.T., Grant-in-Aid for Scientific Research on Innovative Areas [25115502, 23112701] to A.T., Grant-in-Aid for Young Scientists [B] [25870015] to S.S.), IRYO HOJIN SHADAN JIKOKAI (H. Tanaka and N. Takayanagi) to A.T., the Kato Memorial Bioscience Foundation to A.T., the Yasuda Medical Foundation to A.T., the Takeda Science Foundation to A.T., and The Waksman Foundation of Japan to A.T. Y.I. is an employee of PhoenixBio.

Received: June 23, 2014
Accepted: December 3, 2014
Published: December 31, 2014

REFERENCES

Ablasser, A., Bauernfeind, F., Hartmann, G., Latz, E., Fitzgerald, K.A., and Hornung, V. (2009). RIG-I-dependent sensing of poly(dA:dT) through the induction of an RNA polymerase III-transcribed RNA intermediate. Nat. Immunol. *10*, 1065–1072.

Bartenschlager, R., and Schaller, H. (1992). Hepadnaviral assembly is initiated by polymerase binding to the encapsidation signal in the viral RNA genome. EMBO J. *11*, 3413–3420.

Baum, A., Sachidanandam, R., and García-Sastre, A. (2010). Preference of RIG-I for short viral RNA molecules in infected cells revealed by next-generation sequencing. Proc. Natl. Acad. Sci. USA *107*, 16303–16308.

Chiu, Y.H., Macmillan, J.B., and Chen, Z.J. (2009). RNA polymerase III detects cytosolic DNA and induces type I interferons through the RIG-I pathway. Cell *138*, 576–591.

Choi, M.K., Wang, Z., Ban, T., Yanai, H., Lu, Y., Koshiba, R., Nakaima, Y., Hangai, S., Savitsky, D., Nakasato, M., et al. (2009). A selective contribution of the RIG-I-like receptor pathway to type I interferon responses activated by cytosolic DNA. Proc. Natl. Acad. Sci. USA *106*, 17870–17875.

Cui, S., Eisenächer, K., Kirchhofer, A., Brzózka, K., Lammens, A., Lammens, K., Fujita, T., Conzelmann, K.K., Krug, A., and Hopfner, K.P. (2008). The C-terminal regulatory domain is the RNA 5′-triphosphate sensor of RIG-I. Mol. Cell *29*, 169–179.

Fujiwara, K., Tanaka, Y., Paulon, E., Orito, E., Sugiyama, M., Ito, K., Ueda, R., Mizokami, M., and Naoumov, N.V. (2005). Novel type of hepatitis B virus mutation: replacement mutation involving a hepatocyte nuclear factor 1 binding site tandem repeat in chronic hepatitis B virus genotype E. J. Virol. *79*, 14404–14410.

Halegoua-De Marzio, D., and Hann, H.W. (2014). Then and now: the progress in hepatitis B treatment over the past 20 years. World J. Gastroenterol. *20*, 401–413.

Hornung, V., Ellegast, J., Kim, S., Brzózka, K., Jung, A., Kato, H., Poeck, H., Akira, S., Conzelmann, K.K., Schlee, M., et al. (2006). 5′-Triphosphate RNA is the ligand for RIG-I. Science *314*, 994–997.

Huang, L., Hwang, J., Sharma, S.D., Hargittai, M.R., Chen, Y., Arnold, J.J., Raney, K.D., and Cameron, C.E. (2005). Hepatitis C virus nonstructural protein 5A (NS5A) is an RNA-binding protein. J. Biol. Chem. *280*, 36417–36428.

Iwamoto, M., Watashi, K., Tsukuda, S., Aly, H.H., Fukasawa, M., Fujimoto, A., Suzuki, R., Aizaki, H., Ito, T., Koiwai, O., et al. (2014). Evaluation and identification of hepatitis B virus entry inhibitors using HepG2 cells overexpressing a membrane transporter NTCP. Biochem. Biophys. Res. Commun. *443*, 808–813.

Jeong, J.K., Yoon, G.S., and Ryu, W.S. (2000). Evidence that the 5′-end cap structure is essential for encapsidation of hepatitis B virus pregenomic RNA. J. Virol. *74*, 5502–5508.

Junker-Niepmann, M., Bartenschlager, R., and Schaller, H. (1990). A short cis-acting sequence is required for hepatitis B virus pregenome encapsidation and sufficient for packaging of foreign RNA. EMBO J. *9*, 3389–3396.

Kato, H., Orito, E., Gish, R.G., Sugauchi, F., Suzuki, S., Ueda, R., Miyakawa, Y., and Mizokami, M. (2002). Characteristics of hepatitis B virus isolates of genotype G and their phylogenetic differences from the other six genotypes (A through F). J. Virol. *76*, 6131–6137.

Knaus, T., and Nassal, M. (1993). The encapsidation signal on the hepatitis B virus RNA pregenome forms a stem-loop structure that is critical for its function. Nucleic Acids Res. *21*, 3967–3975.

Kotenko, S.V. (2011). IFN-λs. Curr. Opin. Immunol. *23*, 583–590.

Kotenko, S.V., Gallagher, G., Baurin, V.V., Lewis-Antes, A., Shen, M., Shah, N.K., Langer, J.A., Sheikh, F., Dickensheets, H., and Donnelly, R.P. (2003). IFN-lambdas mediate antiviral protection through a distinct class II cytokine receptor complex. Nat. Immunol. *4*, 69–77.

Lu, H.L., and Liao, F. (2013). Melanoma differentiation-associated gene 5 senses hepatitis B virus and activates innate immune signaling to suppress virus replication. J. Immunol. *191*, 3264–3276.

Moeller, A., Kirchdoerfer, R.N., Potter, C.S., Carragher, B., and Wilson, I.A. (2012). Organization of the influenza virus replication machinery. Science *338*, 1631–1634.

Nakagawa, S., Hirata, Y., Kameyama, T., Tokunaga, Y., Nishito, Y., Hirabayashi, K., Yano, J., Ochiya, T., Tateno, C., Tanaka, Y., et al. (2013). Targeted induction of interferon-λ in humanized chimeric mouse liver abrogates hepatotropic virus infection. PLoS ONE *8*, e59611.

Park, H., Serti, E., Eke, O., Muchmore, B., Prokunina-Olsson, L., Capone, S., Folgori, A., and Rehermann, B. (2012). IL-29 is the dominant type III interferon produced by hepatocytes during acute hepatitis C virus infection. Hepatology *56*, 2060–2070.

Pollack, J.R., and Ganem, D. (1993). An RNA stem-loop structure directs hepatitis B virus genomic RNA encapsidation. J. Virol. *67*, 3254–3263.

Protzer, U., Maini, M.K., and Knolle, P.A. (2012). Living in the liver: hepatic infections. Nat. Rev. Immunol. *12*, 201–213.

Rehermann, B., and Nascimbeni, M. (2005). Immunology of hepatitis B virus and hepatitis C virus infection. Nat. Rev. Immunol. *5*, 215–229.

Rehwinkel, J., and Reis e Sousa, C. (2010). RIGorous detection: exposing virus through RNA sensing. Science *327*, 284–286.

Revill, P., and Yuan, Z. (2013). New insights into how HBV manipulates the innate immune response to establish acute and persistent infection. Antivir. Ther. (Lond.) *18*, 1–15.

Saito, T., Hirai, R., Loo, Y.M., Owen, D., Johnson, C.L., Sinha, S.C., Akira, S., Fujita, T., and Gale, M., Jr. (2007). Regulation of innate antiviral defenses through a shared repressor domain in RIG-I and LGP2. Proc. Natl. Acad. Sci. USA *104*, 582–587.

Saito, T., Owen, D.M., Jiang, F., Marcotrigiano, J., and Gale, M., Jr. (2008). Innate immunity induced by composition-dependent RIG-I recognition of hepatitis C virus RNA. Nature *454*, 523–527.

Sheppard, P., Kindsvogel, W., Xu, W., Henderson, K., Schlutsmeyer, S., Whitmore, T.E., Kuestner, R., Garrigues, U., Birks, C., Roraback, J., et al. (2003). IL-28, IL-29 and their class II cytokine receptor IL-28R. Nat. Immunol. *4*, 63–68.

Song, Z.L., Cui, Y.J., Zheng, W.P., Teng, D.H., and Zheng, H. (2012). Diagnostic and therapeutic progress of multi-drug resistance with anti-HBV nucleos(t)ide analogues. World J. Gastroenterol. *18*, 7149–7157.

Sugiyama, M., Tanaka, Y., Kato, T., Orito, E., Ito, K., Acharya, S.K., Gish, R.G., Kramvis, A., Shimada, T., Izumi, N., et al. (2006). Influence of hepatitis B virus genotypes on the intra- and extracellular expression of viral DNA and antigens. Hepatology *44*, 915–924.

Sumpter, R., Jr., Loo, Y.M., Foy, E., Li, K., Yoneyama, M., Fujita, T., Lemon, S.M., and Gale, M., Jr. (2005). Regulating intracellular antiviral defense and permissiveness to hepatitis C virus RNA replication through a cellular RNA helicase, RIG-I. J. Virol. *79*, 2689–2699.

Sun, L., Wu, J., Du, F., Chen, X., and Chen, Z.J. (2013). Cyclic GMP-AMP synthase is a cytosolic DNA sensor that activates the type I interferon pathway. Science *339*, 786–791.

Takahasi, K., Yoneyama, M., Nishihori, T., Hirai, R., Kumeta, H., Narita, R., Gale, M., Jr., Inagaki, F., and Fujita, T. (2008). Nonself RNA-sensing mechanism of RIG-I helicase and activation of antiviral immune responses. Mol. Cell *29*, 428–440.

Takeuchi, O., and Akira, S. (2009). Innate immunity to virus infection. Immunol. Rev. *227*, 75–86.

Tateno, C., Yoshizane, Y., Saito, N., Kataoka, M., Utoh, R., Yamasaki, C., Tachibana, A., Soeno, Y., Asahina, K., Hino, H., et al. (2004). Near completely humanized liver in mice shows human-type metabolic responses to drugs. Am. J. Pathol. *165*, 901–912.

Turelli, P., Mangeat, B., Jost, S., Vianin, S., and Trono, D. (2004). Inhibition of hepatitis B virus replication by APOBEC3G. Science *303*, 1829.

Unterholzner, L., Keating, S.E., Baran, M., Horan, K.A., Jensen, S.B., Sharma, S., Sirois, C.M., Jin, T., Latz, E., Xiao, T.S., et al. (2010). IFI16 is an innate immune sensor for intracellular DNA. Nat. Immunol. *11*, 997–1004.

Wang, H., and Ryu, W.S. (2010). Hepatitis B virus polymerase blocks pattern recognition receptor signaling via interaction with DDX3: implications for immune evasion. PLoS Pathog. *6*, e1000986.

Watashi, K., Liang, G., Iwamoto, M., Marusawa, H., Uchida, N., Daito, T., Kitamura, K., Muramatsu, M., Ohashi, H., Kiyohara, T., et al. (2013). Interleukin-1 and tumor necrosis factor-α trigger restriction of hepatitis B virus infection via a cytidine deaminase activation-induced cytidine deaminase (AID). J. Biol. Chem. *288*, 31715–31727.

Wei, C., Ni, C., Song, T., Liu, Y., Yang, X., Zheng, Z., Jia, Y., Yuan, Y., Guan, K., Xu, Y., et al. (2010). The hepatitis B virus X protein disrupts innate immunity by downregulating mitochondrial antiviral signaling protein. J. Immunol. *185*, 1158–1168.

Wieland, S., Thimme, R., Purcell, R.H., and Chisari, F.V. (2004). Genomic analysis of the host response to hepatitis B virus infection. Proc. Natl. Acad. Sci. USA *101*, 6669–6674.

Yan, H., Zhong, G., Xu, G., He, W., Jing, Z., Gao, Z., Huang, Y., Qi, Y., Peng, B., Wang, H., et al. (2012). Sodium taurocholate cotransporting polypeptide is a functional receptor for human hepatitis B and D virus. eLife *1*, e00049.

Yoneyama, M., Kikuchi, M., Natsukawa, T., Shinobu, N., Imaizumi, T., Miyagishi, M., Taira, K., Akira, S., and Fujita, T. (2004). The RNA helicase RIG-I has an essential function in double-stranded RNA-induced innate antiviral responses. Nat. Immunol. *5*, 730–737.

Yoneyama, M., Kikuchi, M., Matsumoto, K., Imaizumi, T., Miyagishi, M., Taira, K., Foy, E., Loo, Y.M., Gale, M., Jr., Akira, S., et al. (2005). Shared and unique functions of the DExD/H-box helicases RIG-I, MDA5, and LGP2 in antiviral innate immunity. J. Immunol. *175*, 2851–2858.

You, S., and Rice, C.M. (2008). 3′ RNA elements in hepatitis C virus replication: kissing partners and long poly(U). J. Virol. *82*, 184–195.

Yu, S., Chen, J., Wu, M., Chen, H., Kato, N., and Yuan, Z. (2010). Hepatitis B virus polymerase inhibits RIG-I- and Toll-like receptor 3-mediated beta interferon induction in human hepatocytes through interference with interferon regulatory factor 3 activation and dampening of the interaction between TBK1/IKKepsilon and DDX3. J. Gen. Virol. *91*, 2080–2090.